The formation and differentiation of magmas

Bezmen N.I, Gorbachev P.N. Petrochemical types of layered magmatic complexes and modeling ore-forming differentiation trends.

Institute of Experimental Mineralogy RAS, Chernogolovka Moscow district (bezmen@iem.ac.ru)

Abstract. As the main classification feature of igneous complexes, features of the intra-chamber cameral evolution of igneous melts were taken. The rocks of the stratified massifs are combined into differentiation trends, the combination and location of which on the petrochemical diagram determine the type of differentiation. Each differentiation trend corresponds to its own ore specialization. The number and location of array differentiation trends depends not only on the composition of the initial igneous melts, but also on the physicochemical conditions of formation, with the fluid components having a special role.

Keywords: melt, differentiation, experiment, gabbro-syenite, differentiation melts, contrast, cryptic.

Introduction. Many minerals are associated with massifs of magmatic origin, in particular sulfide copper-nickel ores, chromite and titanium-magnetite deposits, deposits of platinum group elements (PGE), etc. besides petrological, also economic value. In this article, petrochemical systematization of igneous complexes was developed, which formed the basis of the petrologometallogenic classification of differentiated intrusions with the separation of massifs that are promising for the content of ore mineralization.

Theoretical analysis. **Method for constructing petrochemical diagrams.** The whole range of rocks of stratified massifs (ultrabasic, basic, acidic, alkaline, and even ore) is compared in the diagram. It is based on the separation of the femic components, salic and silica. Since the role of calcium is dual: on the one hand, it is concentrated together with aluminum, binding in the composition of the main plagioclase, on the other hand, it accumulates together with iron in clinopyroxene, the total calcium content was divided by calculating:
$Ca^{P1}=0.5(Al + Na + K)$, $Ca^{Px} = Ca – 0.5(Al + Na + K)$

The diagram $(Mg+Fe+Mn+C^{Px}+Cr+Ti+P)$ - $(Na+K+Ca^{P1}+Al)$ - Si (in at.%) clearly shows the petrochemical differences of the rocks, since all the main rock-forming elements are used.

Experimental technique. Some interesting trends in liquid nano-cluster differentiation were confirmed experimentally. As a rule, the fluid phase of the massifs contains water, hydrogen, fluorine and other fluid components; therefore, the experiments were carried out in a high-pressure gas equipment with controlled gas fugacity in the H–C–F–Cl system. It's the main components of magmatogenic fluid. The peculiarity of the experimental technique was the direct dosing of hydrogen in the fluid by diffusing it through the walls of platinum ampoules using the improved Shaw membrane technique (Bezmen et al., 2016) and controlling the fugacity of other gases in the H–O–C system with buffer reactions involving carbon or Ni-Fe in the presence of hydrogen-containing wustite. The scheme of a hydrogen cell with a charged ampoule is described in detail in (Bezmen, 2001; Bezmen et al., 2016). As the initial silicate sample, a glass powder prepared from oxides was used, corresponding to the bulk composition of the trend rocks. In order to avoid diffusion of iron into the platinum ampoule from the melt during the experiment, the runs were carried out in glass graphite crucibles, or Ni-Fe alloy, which simultaneously were indicators of carbon activity or oxygen fugacity. Fluorine and chlorine were used in the form of an acid solution. The crucible was inserted into a platinum ampoule with a diameter of 8 mm and a height of 50 mm with a wall thickness of 0.2 mm. Then water was poured into the ampoule, the weight of which was determined by temperature and pressure. The presence of water in the reaction ampoule after the experiment was considered a prerequisite for the reliability of the experiment. The welded capsule was inserted into a Re-reactor, which was filled under a pressure of 100 atm with an argon-hydrogen mixture with a given molar fraction of hydrogen.

Methodological characteristics of experiences, received results and their discussion. *Stratiform complexes.* It was experimentally shown (Bezmen, 1992; Bezmen, 2001) that the composition of the fluid phase has a significant effect on the differentiation of melts. The presence in the fluid phase of carbon-containing gases, especially CH_4, stimulates the separation of ultrabasic melts in the upper parts of the sample. As an example, we present the results of experimental modeling of the basal zone of the Bushveld complex in South Africa. The

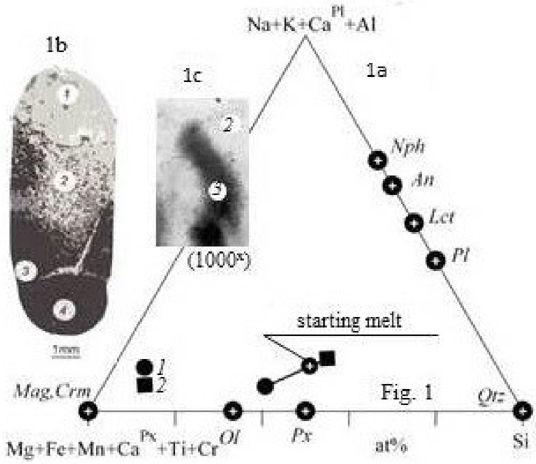

Fig.1.

main role in this part of the section belongs to the dunites and olivine bronzitites containing a small amount of plagioclase. The average composition of this zone (Fig. 1a) is close to plagioclase-containing olivine bronzitite. As the initial composition for experimental modeling glass of the following composition was synthesized from oxides in a high-temperature vacuum furnace at 1700°C (wt.%): SiO_2-49.1; TiO_2-O.2; Al_2O_3-7.56; Fe_2O_3-9.48; FeO-5.36; MnO-0.16; MgO-22.79; CaO-4.52; K_2O-O.11; Na_2O-0.71. The experiments were carried out under the pressure of complex gas mixtures of the H-O-C-S system at P = 4 MPa and T = 1350°C. The mole fraction of hydrogen in the experiment was controlled by an argon-hydrogen mixture and was X_{H2} = 0.2. The fugacity of other gases was determined by the presence of elemental carbon from which the crucible was made, and by the melt of pyrrhotite. The fluid phase at the parameters of the experiment had the following composition: X_{H2O} = 0.31; X_{H2} = 0.2; X_{H2S} = 0.003; X_{CO2} = 0.077; X_{CO} = 0.19; X_{CH4} = 0.218; $\log f_{O2}$ = -9.9; $\log f_{S2}$ == - 3.71. The specified parameters are as close as possible to the formation conditions of the Bushveld complex, in the rocks of which elemental carbon is present (Touysinhthiphonexoy et al., 1984), in gas-liquid inclusions of minerals recovered gases, including CH_4 (Ballhaus, Stuchfl, 1985). Besides, the redox conditions of rock formation are also close to natural (Elliott et al., 1982).

Under the pressure of hydrogen-containing fluids in the absence of a thermal gradient, the initial melt is stratified with accumulation of melt close to the dunite in the upper zone of the crucible, fig. 1b (1). The superliquidus temperatures were confirmed by experiments under pure water pressure (P_{tot} = P_{H2O} = 1200 bar) equal to the partial pressure in mixtures (X_{H2O} = 0.31). After 3 days of the experiment, the upper peridotite zone is represented by large (up to 1 mm) idiomorphic olivine crystals crystallized during quenching, between which there is not intergranular liquid. This zone has the following composition (wt.%): SiO_2 - 42.76; TiO_2 - 0.2; Al_2O_3 - 4.2; FeO - 17.41; MnO - 32.69; CaO - 2.14; K_2O - 0.007; Na_2O - 0.44. The lower zone, transparent glass, has a composition close to plagioclase bronzitite: SiO_2 - 50.80; TiO_2 - O.2; Al_2O_3 - 9.99; FeO - 14.34; MnO - 0.15; MgO - 17.61; CaO - 5.78; K_2O - 0.18; Na_2O - 0.95.

In this zone (2), there is a new fluid separation in the form of packages or spheroids of clusters of macromolecules, Fig. 1b,c (3), which are gravitationally displaced to the bottom of the sample, where they form a liquid enriched with bronzite: SiO_2 - 51.09; TiO_2 - O.2; Al_2O_3 - 9.37; FeO - 15.13; MnO - 0.15; MgO - 18.36; CaO - 4.71; K_2O - 0.17; Na_2O - 0.84. After quenching, it has a tangled - fibrous characteric structure of the devitrified colloidal, macromolecular liquids (Strepikheev, Derevitskaya, 1976). The sulphide melt, fig. 1b (3) was used to determine the H_2S and S_2 fugacity. In general, the initial fluid in the experiment determined the antidromic type of differentiation. Antidromic differentiation is characteristic of the Ural-Alaskan type massifs, the Yelan-Vyazovsky and Podkolodnovsky massifs of the Voronezh crystalline shield, the Burpalinsky massif in Siberia. As a result of migration of volatile components to the upper part of the massif, the composition of the fluid changes, which affects the content and specialization of fluid components in melts of cluster shells (Bezmen, 2001). As a result, in some parts of the section of stratified complexes against the background of homodromic development of rocks, an anti-dromic type of differentiation may occur (for example, in the Khibinsky alkaline massif on the Kola Peninsula).

Gabbro-anorthosite, gabbro-granite and gabbro-syenite massifs. These massifs are characterized by close differentiation trends of plagioclase – alkaline ferrous gabbro – ilmenite - Ti-magnetite ores. They were formed in the zones of activation of the platforms in a relatively quiet tectonic setting and therefore they are contrast layered with separation of rich Ti-magnetite and ilmenite ores (up to 15 wt.% TiO_2). It was experimentally studied the stratification in the Novomirgorodsky (Ukraine) gabbro-anorthosite massif and gabbro-syenite one of the Northern Timan (Kola Peninsula).

Novomirgorodsky gabbro-anorthosite massif. The superliquidus nano-cluster laering of the ore-silicate gabbro melt containing anorthosite gabbro (33 wt.%) and ilmenite (67 wt.%) corresponding to the Novomirgorodsky massif rocks is shown in Fig. 2a Pyroxenites of this massif contain atomic carbon phenocrysts, which indicates the reducing environment for the formation of the selected association of the massif rocks. The experiments were carried out at 1250°C and at a pressure of 400 MPa. A weighed homogeneous powder of start composition (210 mg) was pressed into a glass carbon crucible that was placed in a platinum capsule of ∅ 7 mm. Then a solution (150 mg) of acids (HF -

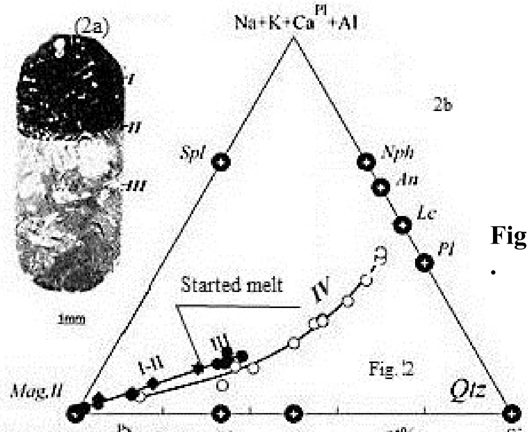

Fig.2
.

0.25 wt.%, HCl - 0.25 wt.%, H_3PO_4 - 0.15 wt.% and H_3BO_3 - 0.15 wt.%) was poured into the capsule and paraffin, C_nH_{n+2} (50 mg), was added. The composition of the fluid phase was controlled by molar fractions of hydrogen (X_{H2} = 0.18) in the argon hydrogen cell of the reactor and atomic carbon of the crucible (Bezmen, Gorbachev, 2017). Within 3 days, the melt was stratified into three compositions: ilmenite (*I*), rutile (*II*) and anortosite gabbro (*III*). The obtained data (*I-III*) practically coincide with the natural trend of differentiation of the studied massif (*IV*).

Gabbgo-Syenite Northern Timan massif. During the experimental interaction of magmatic fluid, which is close to the natural alkaline gabbro-syenitic melt of the Northern Timan massif, several stratified melts of different composition were formed, fig. 3 (2), which in the petrochemical diagram coincide with the trend of differentiation of rocks of the massif (1). *Ti-Mag* mineralization in the form of globules is confined to gabbro-pyroxenites (9.19 wt.% TiO_2) and syenite lenticular separations (5.03 wt.% TiO_2).

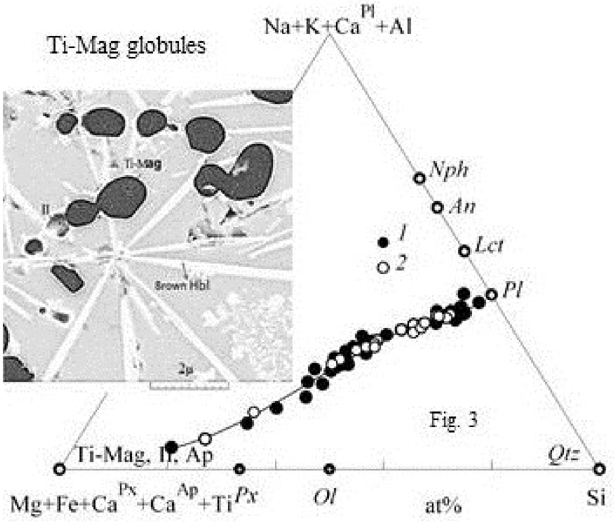

Fig.3.

Chromite ores of stratiform complexes. They are present at various combinations with ultrabasites in the section of massifs and reflect their heterogeneity due to magmatic fluid differentiation. Mineralization is represented by autonomous thick layers or packs of massive monomineral rocks. Very often, ores enter into rhythmic interbedding with basites (dunites, pyroxenites, and sometimes with anorthosites). In general, developing from the dunite-harzburgite ophiolite formations to the dunite-clinopyroxenite rift zones, and then to the stratiform magmatism of the platforms, mineralization changes from chromite to chromite-platinoid (native) and further to chromite-platinoid (sulphide).

An experimental study of the liquid separation of a chromite melt from a silicate melt in the presence of platinum sulfide liquid was carried out at 1250°C under the pressure of a fluid of the H–O–C–S system. Homogeneous glass, fig. 4 (1) anortite-orthopyroxenite composition, $An_{80}Ab_{20}$ (30 wt.%) - $En_{75}Fs_{25}$ (70 wt.%), with an initial content of 0.5 wt. % Cr_2O_3, which is close to the bulk composition of the Merensky Reef of the Bushveld Complex. The experiments were carried out in glass-graphite crucibles, i.e. with carbon activity equal to one. Pyrrhotite (3) was used as an indicator of sulfur fugacity.

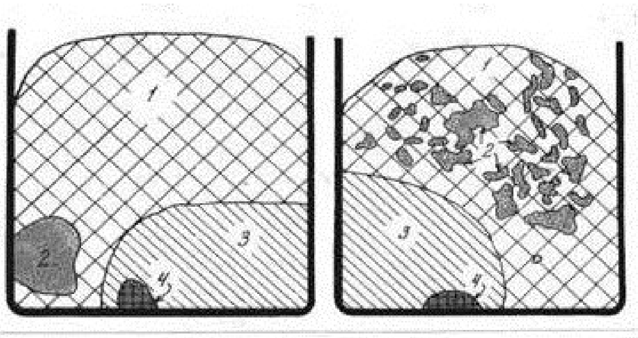

a) b)

Fig.4.

In fig. 4, it can be seen that after 3 days of exposure, the chromite-liquid (17.85 wt.% Cr_2O_3) separated in the lower part of the capsule in the form of an oval-shaped brown glass, fig. 4a (2), or forms irregularly shaped clusters of glass (3.87 wt.% Cr_2O_3), unevenly distributed over the section of the silicate column (Fig. 4 b). Chromium-containing isolations are placed in a semi-transparent glassy matrix of silicate composition and enriched in sulfur (0.8 wt.%) relative to the silicate matrix (0.1-0.2 wt.%). Sulfide melts (3) are enriched with platinum and gold (4), however, the separation coefficients between silicate and chromitic liquids according to neutron activation analysis (Bezmen et al., 1994) are several orders of magnitude lower ($K_D = n\cdot10^{-2}$) than for sulfide-silicate separation ($K_D = n\cdot10^{-3} - n\cdot10^{-5}$).

Conclusions. The supraliquidus nano-cluster differentiation of magmatic melts, crystallization of magmas at different levels of the section, separation of volatile, enriched ore components, and their interaction with the overlying magmas or rocks constitute a complex petrogenetic system of evolution of magmatic chambers. At various stages of this process, concentrations of fluids arise, leading to the separation of ore magmas, regularly associated with specific zones of the section of the massifs. Since the fluid components migrate both by themselves and simultaneously with the fluid-containing shells of the migrating nano-clusters, the effects of stratification further develop under the influence of fluids in the upper part of the magma chamber. In the lower parts of the magmatic chamber, the crystallization processes are activated from bottom to top due to the formation of solidus temperatures as a result of the dissipation of fluid components from the melt.

References:

Bezmen N.I. (2001) The superliquidus differentiation of fluid magmatic melts in reducing conditions as a possible mechanism for the formation of stratified massifs (experimental studies) *Petrology*. 9 (4), 398-416.

Bezmen N.I., Gorbachev P.N., Martynenko V.M. (2016) Experimental study of the effect of water on buffer equilibria magnetite-wustite and wustite-metallic iron. *Petrology* 24 (1), 93–109.

Strepikheev A.A., Derevitskaya V.A. (1976) Fundamentals of the chemistry of high-molecular compounds. M .: Chemistry, 437 p.

Ballhaus C.G., Stumpfl E.F. (1985) Fluid inclusions in the Merensky and Bastard reefs western Bushveld complex (abstract). *Can. Mineral*. **23**, 294.

Bezmen N.I. (1992) Hydrogen in magmatic systems. *Experiment in geosciences* **1** (2), 1-33.

Bezmen N.I, Gorbachev P.N. (2017) Experimental study of gabbro-syenite melt differentiation in superliquidus conditions on the example of Northern Timan massife. *Experiment in Geosciences*. **23** (1), 114-117.

Elliott W.C., Grandstaff D.E., Ulmer G.C., Buntin T., Gold D.P. (1982) An. Intrinstic oxygen fugacity study of platinum-carbon associations in layered intrusions. *Econ. Geol*. **77**, 1439-1510.

Touysinhthiphonexay Y., Gold D.P., Deines P. (1984) Some properties of grafite from the Stillwater complex, Montana and the Bushveld igneous complex, *South Africa Geol. Soc.Am. Abst. Progr.* **16**. 677.

Bychkov D.A., Koptev-Dvornikov E.V. A high-precision algorithm for solving the problem of equilibrium minerals-silicate melt, not accumulating error during the computation process. UDC 552.111: 550.41

M.V. Lomonosov Moscow State University, Faculty of Geology, Moscow (dmibychkov@gmail.com)

Abstract. A new algorithm for finding the equilibrium mineral - melt has been developed. On the one hand, it is focused on the use of thermobarometers developed by us for rock-forming and ore minerals, on the other hand, it is independent of the specific type of thermobarometer. Its other advantage is the presence of a clearly defined objective function, which makes it possible to calculate the equilibrium without relying on the previous state of the system and, accordingly, without accumulating errors.

The sum of squared deviations of the current concentrations of the minals from the concentrations of the minals calculated using thermobarometers was chosen as the target function. Analysis of the shape of the surface of the objective function for a simplified system showed that it has a pronounced ravine character. An attempt to apply methods known from the literature to search for the optimum of the objective function in the complete system failed, apparently due to the appearance of local minima. This forced us to develop our own algorithm for finding the optimum of the objective function.

Keywords: *simulation, algorithm, thermobarometer, silicate melt, equilibrium*

The main goal of our research is the reconstruction of the processes of formation of large stratified base-hyperbasite intrusives. This task is very relevant for modern petrology due to the fact that a large number of mineral deposits are associated with large stratified intrusions - EPG, sulfide polymetallic ores, chromite, magnetite and ilmenite. The largest of them are Bushveld, Stillwater, Great Dyke of Zimbabwe, Skayergaard, Volkovskoye field. In addition, the study of the formation of stratified intrusions can shed light on the problem of magmatic evolution. On the one hand, at present, there is no doubt that the leading process of magmatic evolution is crystallization differentiation. But the dynamics of this process remains acutely debatable.

In our opinion, the most promising way of reconstructing the processes occurring in the chambers of stratified intrusions is mathematical modeling. To build a consistent model of a magmatic object, a combination is needed:

- thermodynamic description of the mineral-melt equilibrium;
- algorithm for finding the phase composition of the magmatic system for a given composition, temperature, pressure and oxygen fugacity
- mathematical description of the flow of heat and matter in the crystallizing massif and its enclosing rocks.

At present, our scientific group has developed thermobarometers describing the composition of olivine, plagioclase, orthopyroxene, clinopyroxene, pigeonite, magnetite, ilmenite, and chrome spinelide in equilibrium with silicate melt (Aryayeva et al., 2016; Aryayeva et al., 2018; Koptev-Dvornikov, Bychkov, 2007; Chernyh, 2017). In addition, a thermobarometer was developed, which allows to determine the temperature and the content of sulfide sulfur in the melt during the separation of sulfide liquid from it (Koptev-Dvornikov et al., 2012). The existing thermobarometers combined with a realistic model (Aryayeva et al., 2016), built using the KOMAGMAT software package (Ariskin, Barmina, 2004), made it possible to accurately calculate the position of the cumulative chrome spinelide in the Burakovsky intrusion (Fig. 1).

Thus, on the one hand, the problem of thermodynamic description of the equilibrium mineral — melt for the main rock-forming and ore minerals can be considered solved. On the other hand, modern software known to us do not allow equilibrium to be found between mineral and melt with arbitrary thermobarometers.

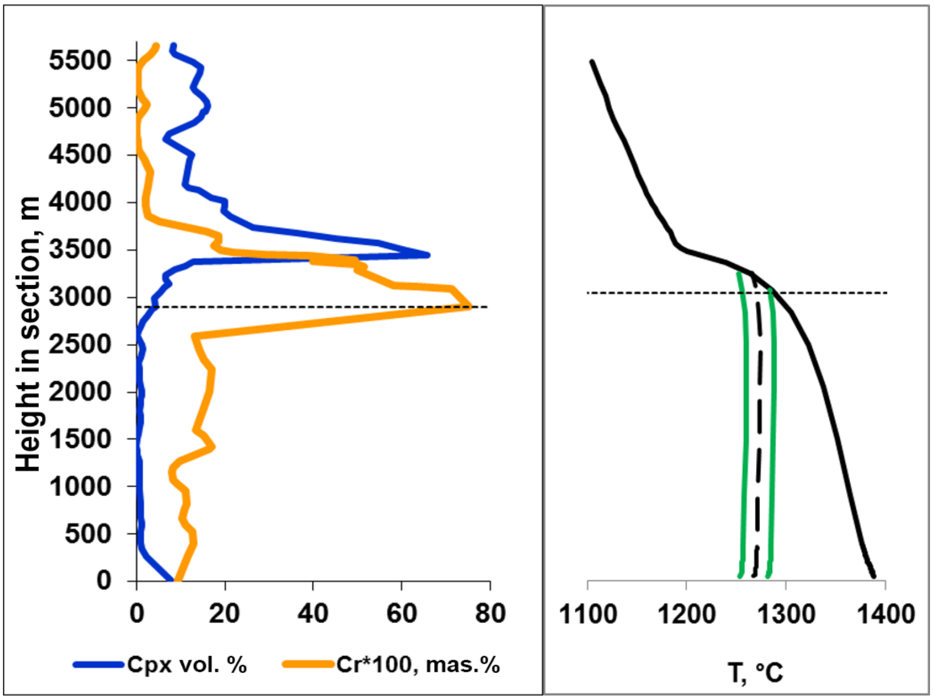

Fig. 1. Comparison of the distribution of the contents of Cr_2O_3 and clinopyroxene in a vertical section of the Burakovsky intrusion with the model temperature and the calculated temperature of the chromspinelide liquidus (Aryayeva et al., 2016).

In addition, in a single program that allows one to describe the crystallization dynamics of an intrusion, the equilibrium search algorithm is constructed in such a way that a computational error accumulates at each calculation step. This state of affairs led us to the decision to develop our own algorithm for finding the phase composition of the magmatic system.

The construction of an algorithm for solving the problem of finding equilibrium is inevitably divided into two subtasks: determining the equilibrium phase composition of the system and calculating the composition and quantity of each of the coexisting phases. It is obvious that the set of coexisting phases is limited by the number of minerals accepted for consideration (the number of liquidus thermobarometers). In our approach to determine the position of the minimum surface of the thermodynamic potential, it is necessary to solve the system of equations of thermobarometers while maintaining the bulk composition of the system at a given temperature and pressure. The solution of such a system of equations involves the determination of a set of phases, their masses and compositions. This solution cannot be found analytically, and for a numerical solution it is necessary to formulate such a function of the system state, the extremum of which corresponds to the equilibrium state.

The selected objective function for the system as a whole is the sum of the objective functions for individual minerals. The type of the objective function for the mineral will become clear from the sequence of its calculation. The initial conditions for calculating the objective function are the given temperature, pressure and phase composition of the system, including the composition of the mineral in question (${}^{giv}X_m^j$ is the mole fraction of the minal m in the given mineral j) and the liquid phase. According to the liquidus thermobarometer, we calculate the mineral composition equilibrium with a given melt (${}^{eq}X_m^j$ is the mole fraction of the minal m in the equilibrium mineral with the melt mineral j calculated by the thermobarometer). The sum of the squares of the differences in the molar fractions of the minals between a given composition of the mineral and the composition of the mineral equilibrated with the given melt is the desired partial value of the objective function F_{obj}^j for the j-th mineral:

$$F_{obj}^j = \sum_{m=1}^{M} ({}^{giv}X_m^j - {}^{eq}X_m^j)^2 \ .$$

Analysis of the shape of the surface of the objective function for minerals - solid solutions showed that it has a curved ravine character. Finding the minimum of the objective function using common algorithms has proven to be ineffective. In this regard, to solve the mineral-melt equilibrium problem, we had to develop an original algorithm.

The homogeneous melt corresponding to the bulk composition of the system is taken as the initial state of the system. The calculation is made for the constant mass of the system. Equilibration of the system begins with the most supersaturated mineral. We consider the mineral with the highest liquidus temperature to be the most supersaturated. The liquidus temperature of a mineral is found by selecting a temperature at which the sum of the mineral minals, calculated using the equations of liquidus thermobarometers, is equal to 1.

The search for the equilibrium mineral-melt is carried out by an iterative method. Each iteration consists of two stages: first, an estimate of the amount of a mineral and then a refinement of its composition.

At the first stage, the amount of the mineral is calculated, at which the sum of the minal contents found will differ from 1 no more than the specified error of quantity calculations (ε_1). For this purpose, the amounts of oxides entering the non-equilibrium phase are subtracted from the initial amount of melt components. They are taken away in proportion corresponding to the ratio of the minals in the mineral and the stoichiometric coefficients at the corresponding oxides. For example, for a plagioclase of composition $An_{80}Ab_{20}$, this proportion is: SiO_2:$AlO_{1.5}$:CaO: $NaO_{0.5}$ as 2.2:1.8:0.8:0.2. The total amount of the mineral with an error not exceeding ε_1 is determined by the Newton method. This completes the first iteration stage (segment 0-1 in Fig. 2).

At point 1, the composition of the mineral corresponds to the composition of the melt at point 0, and the composition of the melt at point 1 is calculated based on the mass balance condition. Thus, these two phases are not consistent.

The content of the second iteration stage consists in changing the mineral composition found at the previous iteration in such a way that it is minimally different from the equilibrium with the melt, while maintaining its amount found at the previous iteration. To do this, using thermobarometers, the composition of the mineral is calculated, equilibrium with the melt at point 1. Then, keeping the sum of moles of the mineral minals, the ratio of the minals changes in accordance with the concentrations found. As a result, the figurative point of the solid phase moves to point 2. To complete the second stage of the next iteration, it is necessary in section 1-2 to find the minimum position of the objective function. Before each new calculation of the target function, the compositions of the mineral and the melt are recalculated in accordance with the mass balance condition.

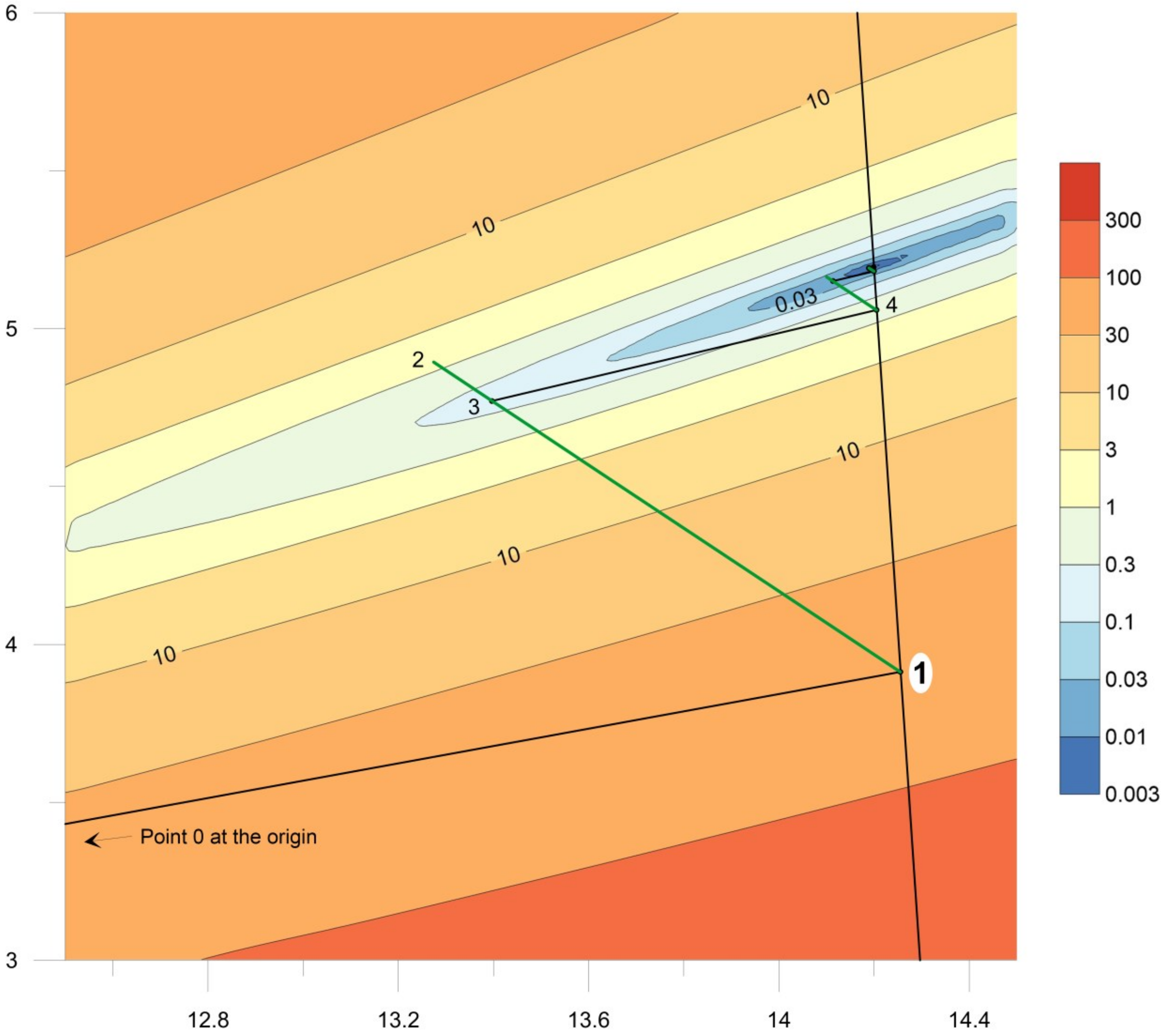

Fig. 2. A graphic representation of the search for a mineral-melt equilibrium. The molar amount of minals is plotted along the axes. The color indicates the value of the objective function.

The search for the minimum is performed by the well-known golden section method. The minimum is considered to be found if the maximum error in estimating the number of minals does not exceed ε_1. Point 3 corresponds to the minimum of the objective function in the interval 1-2. This completes the second stage of the next iteration. Before proceeding to the next iteration, you need to check whether the solution to the problem has already been found, that is, if the required minimum of the objective function has not been found. The solution is considered to be found if the value of the objective function obtained at the next iteration is less than ε_2.

Similarly, the equilibrium between other non-equilibrium minerals and the melt is calculated.

The advantages of the developed algorithm are its independence from the type of thermobarometers describing the mineral-melt thermodynamic equilibrium, the ability to calculate a new state of the system without returning to the initial state of a homogeneous melt, and the independence of the solution from the previous state of the system, that is, no accumulation of errors.

References:

Aryaeva N.S., Koptev-Dvornikov E.V., Bychkov D.A. Liquidus Thermobarometer for Chromite-Melt Equilibrium Modeling: Development and Verification // Moscow University Geology Bulletin. — 2016. Vol. 71, № 5. — pp. 337-346

Aryaeva N.S., Koptev-Dvornikov E.V., Bychkov D.A. A Liquidus Thermobarometer for Modeling of the Magnetite–Melt Equilibrium // Moscow University Geology Bulletin. — 2018. Vol. 73, № 2. — pp. 177-186

Koptev-Dvornikov E.V., Aryaeva N.S., Bychkov D.A. Equation of Thermobarometer for Description of Sulfide–Silicate Liquid Immiscibility in Basaltic Systems // Petrology. — 2012. Vol. 20, № 5. — pp. 450-466

Koptev-Dvornikov E.V., Bychkov D.A. Geothermometers for a wide range of basite compositions // Proceedings of the international conference "Ultrabasic-basic complexes of folded regions". Irkutsk: Publishing House of the Siberian Branch of the Russian Academy of Sciences, 2007. P. 178–181. (in Russian)

Chernykh N.S. The influence of physicochemical parameters on the separation of ore phases from basic magmas (according to the results of mathematical modeling): dis. cand. geol.-min. sci.- M., 2017. (in Russian)

Ariskin A.A., Barmina G.S. COMAGMAT: Development of a magma crystallization model and its petrologic applications // Geochemistry International. — 2004. Vol. 42, №. 1. — pp. 1–157.

Chevychelov V.Y., Virus A. A. Solubility of pyrochlore, microlite and Nb/Ta ratio in granitoid melts at various alkalinity–alumina

UDC 550.42

D.S. Korzhinskii Institute of Experimental Mineralogy of Russian Academy of Sciences (IEM RAS)
(chev@iem.ac.ru)*, (mukhanova@iem.ac.ru)

Abstract. The experiments were conducted in internally heated pressure vessels (IHPV) at *T* = 650, 750 and 850°C, *P* = 100 and 400 MPa and run durations from 4 to 10 days. At pyrochlore dissolution in granitoid melts at *P* = 100 MPa, the highest Nb contents (from 0.7 to 1.9 wt.%) were obtained in alkaline melts (mol. $Al_2O_3/(CaO + Na_2O + K_2O)$ = A/CNK = 0.62-0.63), the content of Nb was decreased to 0.06 -0.38 wt.% in sub-aluminous melts (A/CNK = 1.06 - 1.11) and then slightly was increased to 0.11 - 0.41 wt.% in high-aluminous melts (A/CNK ~ 1.4 -1.7). Temperature increase also has significant positive effect on the pyrochlore solubility. In experiments at increased pressure of 400 MPa, the effect of alkalinity-aluminous content in the melt on the pyrochlore solubility is reduced. The highest contents of Nb (~ 0.86 wt.%) and Ta (~ 0.61 wt.%) were obtained in alkaline granitoid melts (A/CNK = 0.69), the contents of Nb and Ta were significantly (3-5 times) reduced to 0.18 and 0.24 wt.% in sub-aluminous melts (A/CNK = 1.05–1.07) and then again were increased by approximately one and a half to two times to 0.27 wt.% Nb and 0.47% Ta in high-aluminous melts (A/CNK = 1.33 - 1.43). It is shown that pyrochlore is unstable at magmatic conditions in high-aluminous granitic melts. At microlite dissolution in granitoid melts the Nb/Ta ratio in the melt is increase approximately doubles with increasing of the alumina content in the melt (A/CNK ratio increasing from ~1.1 to ~1.4), while at tantalite and columbite dissolution in granitoid melts the Nb/Ta ratio is markedly decrease.

Keywords: *solubility; pyrochlore; microlite; experiment; aluminosilicate melts; granitoids; niobium; tantalum; Nb/Ta ratio*

The initial model glasses of the SiO_2-Al_2O_3-Na_2O-K_2O composition with mol. $Al_2O_3/(Na_2O+K_2O)$ ratios equal to ~0.64, ~1.10 and ~1.70 were melted from gel mixes. Pyrochlore, $(Ca_{1.1}Na_{0.8}La_{0.05}Ce_{0.05})(Nb_{1.8}Ti_{0.2})O_{5.9}F_{1.1}$, from the Vishnevogorsk niobium deposit, as well as OH,Ca-microlite, $(Ca_{1.32}Na_{0.19}Bi_{0.03}Mn_{0.03}Mg_{0.02})(Ta_{1.68}Nb_{0.18}Ti_{0.08}Fe_{0.06})(O,OH)_{5.67}F_{0.33}$, from the state of Minas Gerais, Brazil were used for our experiments.

At the preparation of the experiments, powder of model aluminosilicate glass was filled in Pt capsule, one rather large fragment of a crystalline mineral was placed in the center, 0.2N HF solution (from 4 to 40 wt.%) was added and then the capsule was welded. The experiments were carried out in internally heated pressure vessels (IHPV) at *T* = 650, 750 and 850°C, *P* = 100 and 400 MPa and run durations of 4 to 10 days depending on *T* and *P*.

At pyrochlore dissolution in granitoid melts at *P* = 100 MPa (Fig. 1), the highest Nb contents (from 0.7 to 1.9 wt.%) are representative of alkaline melt (mol. $Al_2O_3/(CaO+Na_2O+K_2O)$ = (A/CNK) = 0.62 -

0.63), the content of Nb decreases to 0.06 -0.38 wt.% in sub-aluminous melt (A/CNK = 1.06 -1.11) and then slightly increases to 0.11 - 0.41 wt.% in high-aluminous melt (A/CNK ~1.4 -1.7). The temperature increase also has significant positive effect on the pyrochlore solubility. The content of Nb in the melt is maximally at $T = 850°C$, and it gradually decreases at T = 750 and 650°C, respectively, in the above ranges. Comparison with our previously obtained results shows (Fig. 2) that at pyrochlore dissolution (~67 wt.% Nb_2O_5) the Nb content in the melt is several times lower than at columbite dissolution (~58 wt.% Nb_2O_5) (Chevychelov et al., 2010; Chevychelov, 2013) and even much lower than at tantalite dissolution (~38 wt.% Nb_2O_5) (Chevychelov, 2016). However the type of dependence of the Nb content on the melt alkalinity-alumina remains the same: the Nb content is maximally in the alkaline melt and it decreases at increasing of alumina content. Moreover the pyrochlore line on the Fig. 2 in the range of A/CNK ~0.6 -1.1 is practically parallel to the dependencies for columbite and tantalite. Pyrochlore becomes unstable at further increase alumina content in melt (A/CNK ~1.45), and the mineral composition begins to change in the near-contact marginal zone (Fig. 3). Primarily Na, F and, to a lesser extent, Ca are removed from pyrochlore, and the mineral becomes impregnated with granitoid melt like a sponge. The melt flows into among the small "islands" of pyrochlore, and it dissolves the mineral.

In pyrochlore instability condition the Nb content in the melt markedly increases. Thus it has been experimentally shown that pyrochlore is unstable in high-aluminous granitic melts at magmatic conditions (T = 650-850°C, P = 100 MPa). At the same time this mineral can crystallize from enriched Ca, Na and F residual alkaline magmatic melts more likely than columbite and tantalite, since the crystallization of pyrochlore requires significantly lower Nb saturation concentration of melt.

In experiments at elevated pressure (400 MPa) the effect of alkalinity-alumina of the melt on the solubility of pyrochlore is reduced (Fig. 4). The highest contents of Nb (~0.86 wt.%) and Ta (~0.61 wt.%) are representative of alkaline granitoid melts (A/CNK = 0.69), the contents of Nb and Ta are significantly (3-5 times) reduced to 0.18 and 0.24 wt.%, respectively, in sub-aluminous melts at A/CNK = 1.05 -1.07, and then they increases again by about one and a half to two times to 0.27 wt.% Nb and 0.47% Ta in high-aluminous melts at A/CNK = 1.33 -1.43. In general, the trends of Nb contents in the melt at pyrochlore dissolution and of Ta contents at microlite dissolution are quite close to each other within the error of determination. The trend of Nb contents in the melt at microlite dissolution is also similar by its shape to the two above studied trends, but it has lower contents about order of magnitude, which is due to low concentrations of Nb in the microlite.

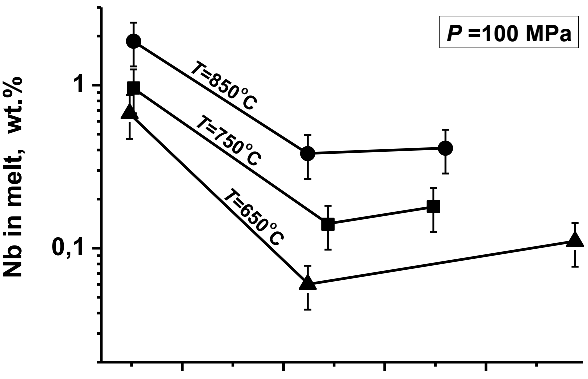

Fig. 1. Temperature dependences of Nb content in granitoid melts with various alkalinity-alumina content at pyrochlore dissolution in the melt.

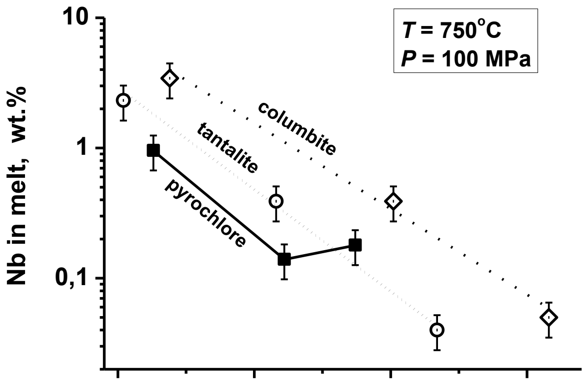

Fig. 2. The Nb content in aluminosilicate melts with various alkalinity-alumina content at pyrochlore dissolution in the melt. For comparison, our previously obtained data on the columbite and tantalite dissolution are represented.

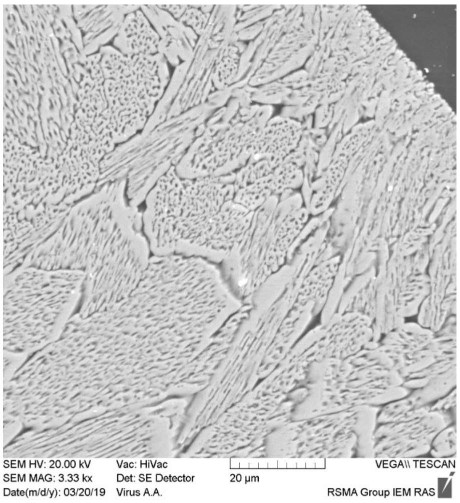

Fig. 3. Decomposition (instability) of pyrochlore in high-aluminous granitic melt (A/CNK ~1.45) at T = 850oC and P = 100 MPa. Na, F and, to a lesser extent, Ca are removed from pyrochlore, and the mineral becomes impregnated with granitoid melt like a sponge.

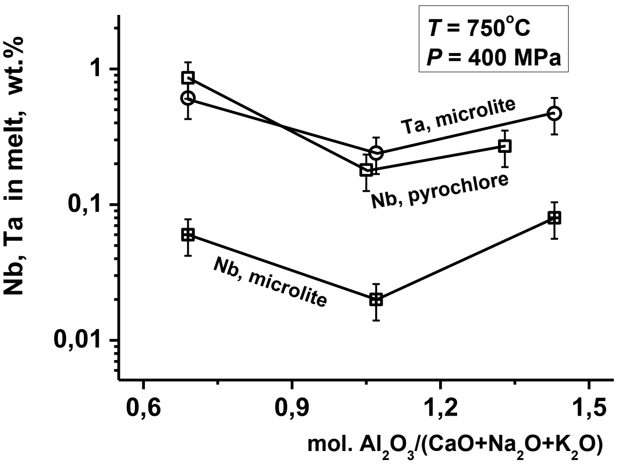

Fig. 4. The contents of Nb and Ta in aluminosilicate melts with various alkalinity-alumina content at the pyrochlore or microlite dissolution in the melt.

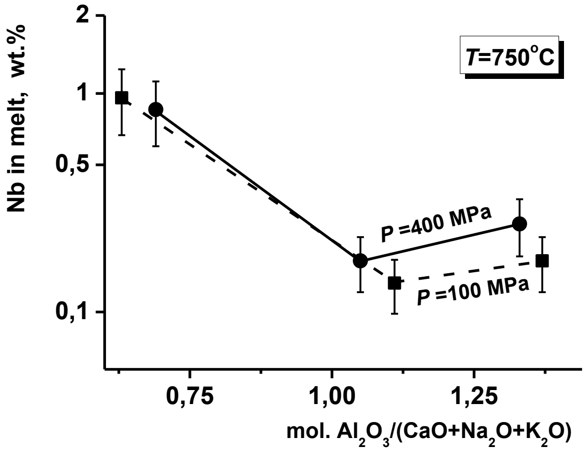

Fig. 5. The Nb content in aluminosilicate melts with various alkalinity-alumina content at pyrochlore dissolution in the melt.

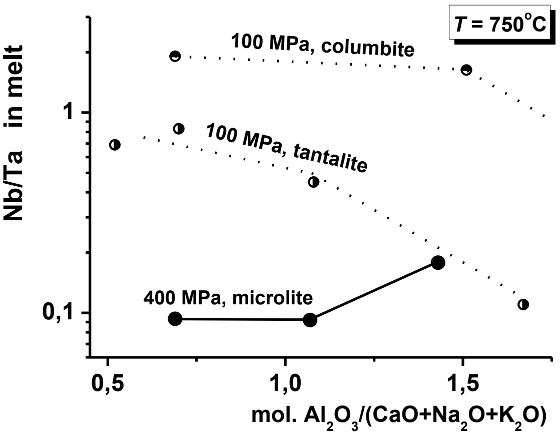

Fig. 6. The Nb/Ta ratios in aluminosilicate melts with various alkalinity-alumina content at microlite dissolution in the melt. For comparison, our data on the columbite and tantalite dissolution are represented**.**

It has not been established that the pressure increase from 100 to 400 MPa at *T* = 750°C has noticeable effect on the Nb content in granitoid melts at pyrochlore dissolution (Fig. 5). The lines of the Nb contents at these two pressures are quite close to each other within the error of determination. At *P* = 400 MPa pyrochlore also becomes unstable in the near-contact marginal zone in high-aluminous melt. In contrast to pyrochlore, the microlite is stable at dissolution in high-aluminous melt, and it does not change its composition in the marginal zone. At microlite and pyrochlore dissolution in high-aluminous melt the Nb and Ta contents increase relative to them contents in the sub-aluminous melt, while at columbite and tantalite dissolution these contents decrease. Apparently, the deficit in the first place Na, and possibly Ca, K in high-aluminous melts increases the pyrochlore and microlite dissolution in these melts.

It was shown that at microlite dissolution the Nb/Ta ratio in the melt changes in other way than at columbite and tantalite dissolution (Fig. 6). So, at the A/CNK ratio in the melt increase (from ~1.1 to ~1.4) the Nb/Ta ratio enhance approximately doubles, while at tantalite and columbite dissolution the Nb/Ta ratio noticeably decreases.

Acknowledgments. *The authors are grateful to N.V. Chukanov for the kindly provided samples of pyrochlore and microlite.* This study was financially supported by the RFBR, project No 18-05-01001A.

References:

Chevychelov V.Yu. Partitioning of volatile, rock-forming and ore components in magmatic systems: experimental studies: Author's abstract dis. doctor geol.-min. sciences. – Moscow, 2013. - 62 p. (in Russian)

Chevychelov V.Yu. Experimental study of the dissolution of columbite and tantalite-columbite in water-saturated granitoid melts // Sofia Initiative Preservation of Mineral Diversity. VIII International Symposium Mineral diversity research and preservation. Earth and Man National Museum, - Sofia, Bulgaria, 2016. - P. 22-34. (in Russian)

Chevychelov V.Yu., Borodulin G.P., Zaraisky G.P. Solubility of columbite, $(Mn,Fe)(Nb,Ta)_2O_6$, in granitoid and alkaline melts at 650-850°C and 30-400 MPa: an experimental investigation // Geochemistry International. - 2010. – Vol. 48, № 5. - P. 456-464. (in English)

Chevychelov V.Y. On the solubility of natural Nb-containing loparite in granitic model aluminosilicate melts of various composition UDC 550.42

D.S. Korzhinskii Institute of Experimental Mineralogy of Russiani Academy of Sciences (IEM RAS) (chev@iem.ac.ru),

Abstract. Synthetic haplogranitic (SiO_2-Al_2O_3-Na_2O-K_2O) glasses with mol. $Al_2O_3/(Na_2O+K_2O)$ ratios equal to ~0.64, ~1.10 and ~1.70, as well as Nb-containing loparite from pegmatites of the Lovozero massif of the Kola Peninsula $(Na,Ce,La,Ca,Nd)(Ti,Nb)O_3$, containing ~21-25 wt.% Nb_2O_5, were used for our experiments. The experiments were conducted in internally heated pressure vessel (IHPV) at T = 850°C, P = 100 MPa and run duration of 5 days. Quantitative experimental data on the solubility of Nb-containing loparite in high-aluminous, sub-aluminous and alkaline granitoid melts were obtained. The results are compared with the data on the solubility of other tantalum-niobates. It is shown that at loparite dissolution, the Nb content in the melt is significantly lower than at other Nb-containing minerals dissolution. The maximum concentration of Nb is obtained in alkaline melt. This concentration decreases with increasing of aluminous content in the melt. At loparite dissolution in the melt Ce and La behave like Nb, but their content in the melt is lower than Nb. Loparite is unstable in sub-aluminous and high-aluminous melts. The composition of the mineral changes in the near-contact marginal zone, mainly due to the removal of Na.

Keywords: *solubility; loparite; experiment; aluminosilicate melts; granitoids;* niobium; cerium; lanthanum; titanium

Synthetic, prepared from gel mixtures, haplogranitic (SiO_2-Al_2O_3-Na_2O-K_2O) glasses with mol. $Al_2O_3/(Na_2O+K_2O)$ ratios equal to ~0.64, ~1.10 and ~1.70, as well as Nb-containing loparite from pegmatites of the Lovozero massif of the Kola Peninsula $(Na,Ce,La,Ca,Nd)(Ti,Nb)O_3$, containing ~21-25 wt.% Nb_2O_5, were used for our experiments (Table 1).

At the preparation of the experiments, powder of model aluminosilicate glass was filled in Pt capsule, one rather large fragment of crystalline loparite was placed in the center, 0.1N HF solution (~20 wt.%) was added and then the capsule was welded. The experiments were conducted in internally heated pressure vessel (IHPV) at T = 850°C, P = 100 MPa and run duration of 5 days. The specimens for the study by the method of local X-ray spectral analysis were prepared from the obtained samples. The analysis was performed along the profiles perpendicular to the boundary of crystal, melted into glass (Fig. 1). As a result, the solubilities of loparite in granitoid melts at these conditions were calculated, namely, the maximum concentrations of Nb in the melts directly at the boundary with the crystal. The chemical compositions of granitoid melts after the experiments are represented in Table 2.

Quantitative experimental data on the solubility of Nb-containing loparite in high-aluminous, sub-aluminous, and alkaline granitoid melts were obtained. The results are compared with the data on the solubility of other tantalum-niobates (Fig. 2) (Chevychelov, 2013; 2016; 2018; Chevychelov et al., 2010). It is shown that at loparite dissolution, the Nb content in the melt is significantly lower than at other Nb-containing minerals dissolution. However the type of dependence of the Nb content on the melt alkalinity-alumina remains the same: the Nb content is maximally in the alkaline melt and it decreases with increasing of alumina content. At loparite dissolution in the melt cerium and lanthanum behave like niobium (Fig. 3), but their content in melts is even lower than Nb.

Table 1. The chemical composition of loparite after experiments (wt.%, normalized to 100 %).

Chemical composition	F	Na_2O	CaO	TiO_2	Nb_2O_5	La_2O_3	Ce_2O_3	Nd_2O_3	O = F
Initial composition of loparite. Unchanged center of grain	0	10.4	2.2	36.1	23.4	10.6	15.2	2.1	0
Changed marginal zone in sub-aluminous melt	0.2	0.8	3.0	39.6	25.6	11.7	17.1	1.9	0.4
Changed marginal zone in high-aluminous melt	0.2	0.5	2.1	40.1	25.8	11.4	17.5	2.4	0.4

Table 2. The chemical composition of granitoid melts after experiments (wt.%, normalized to 100 %).

Chemical composition	F	Na_2O	Al_2O_3	SiO_2	K_2O	CaO	O = F	A/CNK*
Alkaline melt (initial A/NK ~0.64)	0.7	6.5	11.6	75.9	5.0	0.3	1.2	0.69
Sub-aluminous melt (initial A/NK ~1.10)	0.3	6.1	15.8	73.5	4.0	0.3	0.4	1.05
High-aluminous melt (initial A/NK ~1.70)	0.5	5.5	17.9	72.6	3.2	0.4	0.9	1.36

*A/CNK - alumina coefficient, mol. $Al_2O_3/(CaO+Na_2O+K_2O)$ ratio.

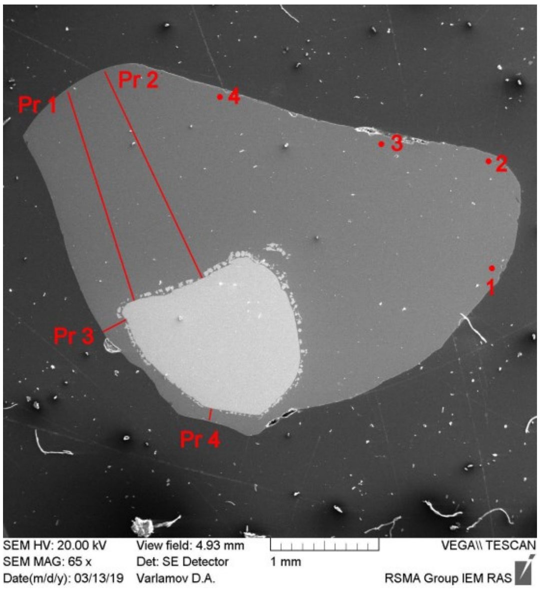

Fig. 1. The polished section of sample after the experiment on the loparite dissolution in alkaline melt.

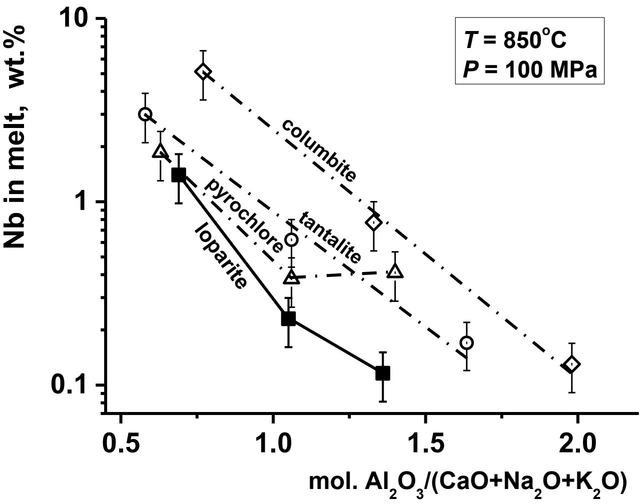

Fig. 2. The Nb content in aluminosilicate melts with various alkalinity-alumina content at loparite dissolution in the melt. For comparison, our previously obtained data on the columbite, tantalite, and pyrochlore dissolution are represented (Chevychelov, 2013; 2016; 2018; Chevychelov et al., 2010).

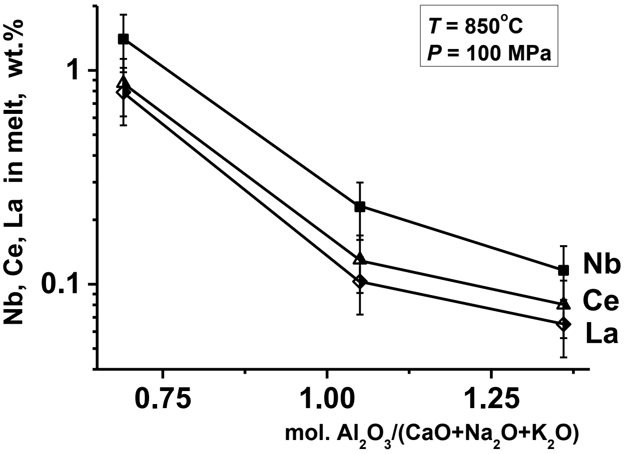

Fig. 3. The contents of Nb, Ce and La in aluminosilicate melts with various alkalinity-alumina content at loparite dissolution in the melt.

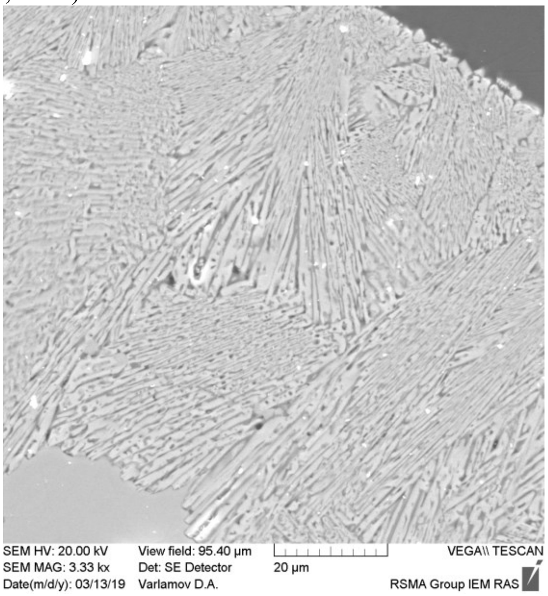

Fig. 4. Decomposition (instability) of loparite in sub-aluminous granitoid melt (A/CNK ~1.05) at $T = 850^{o}C$ and $P = 100$ MPa. Na is removed from loparite in the near-contact marginal zone, and the mineral becomes impregnated with granitoid melt like a sponge.

Loparite, being used in our experiments, is unstable in sub-aluminous and high-aluminous melts. The composition of the mineral changes in the near-contact marginal zone, mainly due to the removal of

Na (Table 2). The mineral becomes impregnated with granitoid melt like a sponge. The melt flows into among the small "islands" of loparite, and it dissolves the mineral (Fig. 4).

Acknowledgments. *The author is grateful to I.V. Pekov for the kindly provided samples of loparite and other tantalum-niobates.* This study was financially supported by the RFBR, project No 18-05-01001A.

References:

Chevychelov V.Yu. Partitioning of volatile, rock-forming and ore components in magmatic systems: experimental studies: Author's abstract dis. doctor geol.-min. sciences. – Moscow, 2013. - 62 p. (in Russian)

Chevychelov V.Yu. Experimental study of the dissolution of columbite and tantalite-columbite in water-saturated granitoid melts // Sofia Initiative Preservation of Mineral Diversity. VIII International Symposium Mineral diversity research and preservation. Earth and Man National Museum, - Sofia, Bulgaria, 2016. - P. 22-34. (in Russian)

Chevychelov V.Yu. Study of solubility of natural pyrochlore in granitoid melts. First experimental results // Experiment in Geosciences. - 2018. - Vol. 24, No 1. - P. 221-222. (in English)

Chevychelov V.Yu., Borodulin G.P., Zaraisky G.P. Solubility of columbite, $(Mn,Fe)(Nb,Ta)_2O_6$, in granitoid and alkaline melts at 650-850^{o}C and 30-400 MPa: an experimental investigation // Geochemistry International. - 2010. – Vol. 48, № 5. - P. 456-464. (in English)

Kotelnikov A.R., Korzhinskaya V.S., Suk N.I., Van K.V., Virus A.A. Experimental study of zircon and loparite solubility in silicate melts UDC 550.89

Institute of Experimental Mineralogy RAS
(kotelnik@iem.ac.ru; vkor@iem.ac.ru; sukni@iem.ac.ru

Abstract. The solubility of zircon in an aluminosilicate melt was experimentally investigated at T = 1000°C and P=2 kbar in the presence of water or a solution of 1M KF. In the experiments, zircon synthesized under hydrothermal conditions and previous melted aluminosilicate glasses with different agpaiticity (from 0.81 to 2.5) were used. It is shown that with an increase in the agpaitic coefficient (K = (Na + K) / Al) of the melt, the solubility of zircon increases 10 or more times (with maximum agpaiticity). The solubility of loparite in an aluminosilicate melt of different composition was studied experimentally at T=1200 and 1000°C and P=2 kbar in dry conditions and in the presence of 10 wt.% H_2O. The initial material was synthetic glass of malignite and eutectic albite-nepheline composition, as well as natural loparite of the Lovozerskiy massif. It is established that the solubility of loparite depends on the composition of the aluminosilicate melt.

Keywords: *silicate melt, zircon, loparite, solubility, experiment*

Experimental method The solubility of zircon and loparite in an aluminosilicate melt was experimentally investigated at T=1000°C and P=2 kbar in a high gas pressure vessel. The installation is characterized by the accuracy of setting and determining the temperature and pressure, large working volume, high performance and considerable duration of experiments. A heater with tungsten-rhenium or molybdenum wire as a heating element allows experiments to be carried out at temperatures up to 1400°C. The temperature was controlled and monitored with Pt-PtRh10 thermocouples with an accuracy of ± 2°C, the pressure was measured with a spring pressure gauge with an error of ± 1%. The gradient free zone is 50 mm, the working diameter of the furnace is 15 mm. The experiments were conducted in welded platinum ampoules, where the sample was placed and, if necessary, the initial solution was poured.

The solubility of zircon was studied in the presence of water or a solution of 1M KF. The duration of the experiments was 5 days. In the experiments, zircon synthesized under hydrothermal conditions and granite (Orlovka deposit, well 42) of the following composition were used (mas.%): SiO_2 – 72.10; TiO_2 – 0.01; Al_2O_3 – 16.14; Fe_2O_3 – 0.68; MnO – 0.09; CaO – 0.30; MgO – 0.01; Na_2O – 5.17; K_2O – 4.28; P_2O5 – 0.02; F – 0.32; H_2O – 0.18, which was previously melted at atmospheric pressure and a temperature of 980°C. Also aluminosilicate glasses with different agpaitic coefficient K_{agp}=(Na+K)/Al (from 0.80 to 2.5) were previously prepared by melting. The experiments were carried out in 7x0.2x50 mm platinum ampoules, into which about 50 mg of granite glass, 5 mg of zircon crystals and about 15 mg of water or 1 M KF were loaded. Ampoules were hermetically sealed and placed in a "gas bomb" for the experiment. The duration of such experiments was 5 days.

The solubility of loparite was studied under dry conditions and in the presence of 10 wt.% H_2O. The duration of the experiments was 1 day. The initial material was synthetic glass of malignite, urtite and eutectic albite-nepheline composition, previously melted at T=1450°C in a furnace with chromite-lanthanum heaters in platinum crucibles for 2 hours, and also natural loparite of the Lovozerskiy massif.

The compositions of all samples after experiments were determined by electron probe X-ray spectral analysis (EZRSA) using a Tescan Vega II XMU scanning electron microscope (Tescan, Czech Republic) equipped with the INCA Energy 450 X-ray microanalysis system with energy-dispersion (INCAx-sight) and crystal diffraction (INCA wave 700) X-ray spectrometers (Oxford Instruments, England) and software platform INCA Energy +.

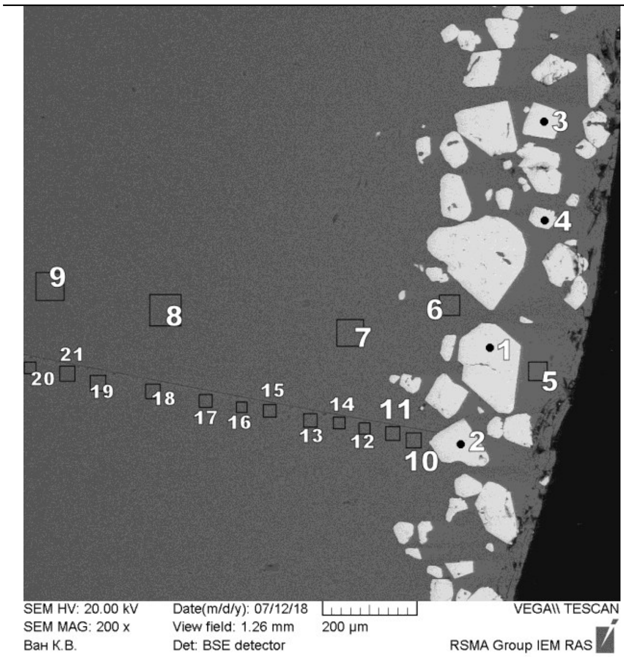

Fig. 1. Diffusion profile in the study of zircon solubility in an aluminosilicate melt in the presence of 1 M KF (T=1000°C, P=2 kbar).

Zircon solubility in an aluminosilicate melt at T= 1000^{o}C, P=2 kbar To estimate the solubility of zircon in an aluminosilicate melt, we used the method of measuring the diffusion profile of the ZrO_2 content in quenching glass from the boundary of the zircon crystal. Figure 1 shows the selected diffusion profile, and fig. 2 shows an example of the measured diffusion distribution profile of ZrO_2 when zircon is dissolved in a granitic melt in the presence of 1 M KF. The figure clearly shows that at a distance of ~ 200 µm, the ZrO_2 content in the glass remains constant and then begins to decrease. This gives grounds to take these maximum values as the solubility of ZrO_2 in the melt.

To determine the effect of agpaiticity on the solubility of zircon in an aluminosilicate melt, experiments were carried out in systems with different K_{agp}=(Na+K)/Al: from 0.80 to 2.5 in the presence of water. The dependence of the solubility of ZrO_2 in the melt on agpaiticity was revealed: with an increase in K_{agp} from 0.8 to 2.08, the solubility of ZrO_2 in glass increases from 0.2 wt.% to 6.54 wt.%. (Fig. 3).

Loparite solubility in an aluminosilicate melt at T=1000°C, P=2 kbar In the course of the experiments, the aluminosilicate melt was saturated with elements characteristic of loparite. At the same time, the formation of titanium-silicates of rare earths was observed, and in water-containing systems – the growth of rims depleted in titanium and enriched in rare-earth elements on loparite crystals. Apparently, this may indicate incongruent dissolution of loparite.

The solubility of loparite can be estimated by determining the sum of oxides of rare earths (La_2O_3, Ce_2O_3, Nd_2O_3) and oxides of elements inherent only in loparite (TiO_2, Nb_2O_5, SrO) in glass obtained as a result of the experiment. The presence of water on the solubility of loparite had almost no effect. It is established that the solubility of loparite depends on the composition of the aluminosilicate melt (Fig. 4, 5): it increases with increasing agpaiticity ((Na+K)/Al) and decreases with increasing Ca/(Na+K) ratio. According to preliminary data, the solubility of loparite in the melt of the malignite composition according to estimates is on average ~ 6.58 wt. %, in the melt corresponding to the composition of albite-nepheline eutectic – on average ~ 5.19 wt. %, and in the melt corresponding to the composition of urtite – 3.7.

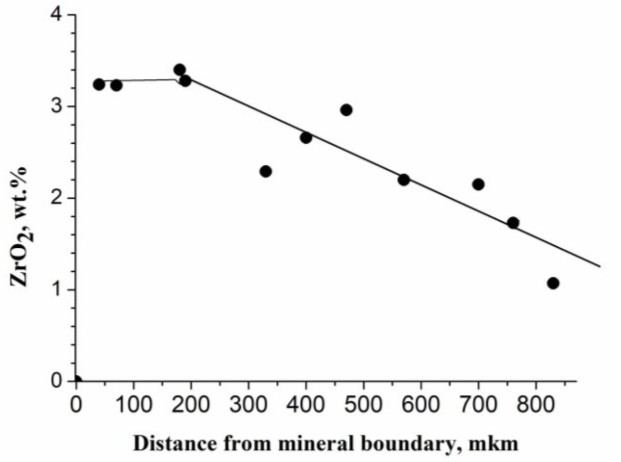

Fig. 2. An example of the measured profile of the diffusion ZrO_2 distribution upon dissolution of zircon in the granite melt with 1 M KF (Kagp=0.80, T=1000°C, P=2 kbar).

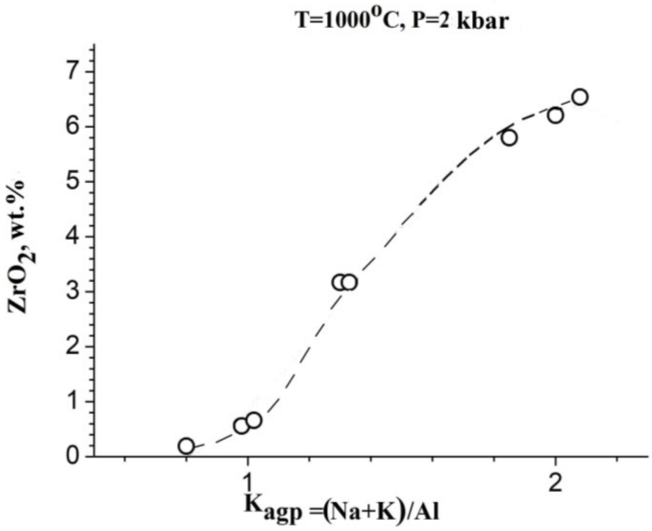

Fig. 3. Dependence of zircon solubility in an aluminosilicate melt in the presence of water on agpaiticity (Kagp=(Na+K)/Al).

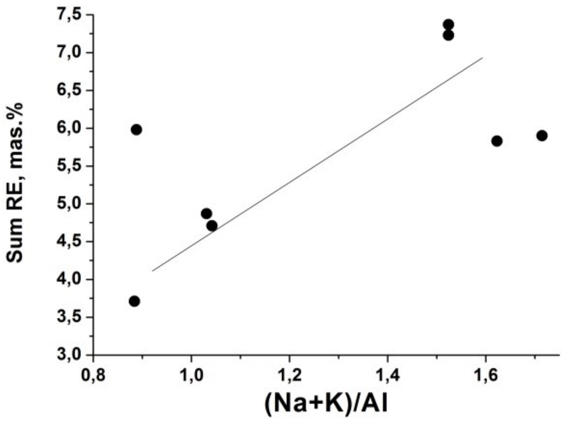

Fig. 4. Dependence of loparite solubility on agpaiticity of aluminosilicate melt ((Na+K)/Al). Sum RE = TiO_2 + Nb_2O_5 + SrO + La_2O_3 + Ce_2O_3 + Nd_2O_3.

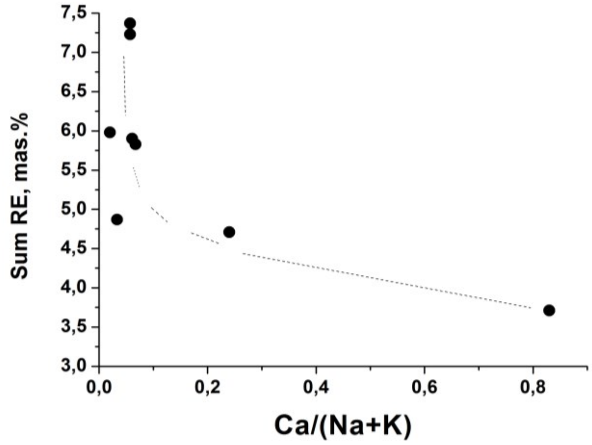

Fig. 5. Dependence of loparite solubility on Ca/(Na+K) of aluminosilicate melt. Sum RE = TiO_2+Nb_2O_5+SrO+La_2O_3+ Ce_2O_3+ Nd_2O_3.

Such values of solubility are not enough to explain the content of loparite in the malignite horizon, to which rich loparite ores are confined. The content of loparite in malignite reaches 20-25%. The data obtained may explain the presence of accessory loparite in the rocks.

In water containing systems, the formation of an emulsion is also observed, which is expressed in the presence of small droplets enriched with elements characteristic of loparite. Apparently, this is a manifestation of titanate-silicate liquid immiscibility (Suk, 2007), which was previously obtained in water containing aluminosilicate systems containing ore elements (Ti, Nb, Sr, REE).

Thus, the formation of rich loparite ores can be explained only by the appearance of titanate-silicate immiscibility, as a result of which the magmatic melt is significantly enriched in ore components.

Reference:

Suk N.I. Experimental study of alkaline magmatic aluminosilicate systems: implication for the genesis of REE-Nb loparite deposits. Dokl. Earth. Sci. V. 414. No 1. P. 615-618.

Kotelnikov A.R.[1], Shapovalov Yu.B.[1], Suk N.I.[1], Kotelnikova Z.A.[2], Korzhinskaya V.S.[1] Liquid immiscibility and problems of ore genesis UDC 550.89:553.062

[1]Institute of Experimental Mineralogy RAS (IEM RAS), Chernogolovka Moscow district, (kotelnik@iem.ac.ru; shap@iem.ac.ru; sukni@iem.ac.ru; vkor@iem.ac.ru);
[2]Institute of Geology of Ore Deposits, Petrography, Mineralogy, and Geochemistry RAS (IGEM RAS), Moscow (kotelnik@igem.ac.ru)

Abstract. The results of an experimental study of phase relations and distribution of elements in the systems of silicate melt – salt (carbonate, phosphate, fluoride, chloride) melt, silicate melt I – silicate melt II, as well as in fluid-magmatic systems in the presence of alkali metal fluorides are presented. Salt extraction of a number of ore elements (Y, REE, Sr, Ba, Ti, Nb, Zr, Ta, W, Mo, Pb) was studied in liquid immiscibility processes in a wide temperature range of 800–1250°C and pressure of 1–5.5 kbar. It is shown that the partition coefficients are sufficient for the concentration of ore elements in the quantity necessary for the genesis of ore deposits. In the fluid-saturated trachyrhyolite melt, separation into two silicate liquids was obtained, and the partition coefficients for a number of elements (Sr, La, Nb, Fe, Cr, Mo, K, Rb, Cs) between phases L1 and L2 were determined. The processes of interaction of a heterophase fluid in the granite (quartz) - ore mineral - heterophase fluid (Li, Na, K-fluoride) system were studied at 650–850°C and P =1 kbar. The formation of a phase of a highly alkaline fluid-saturated silicate melt – Ta and Nb concentrator – is shown as a result of the reaction of the fluid with the rock and ore minerals.

Keywords*: liquid immiscibility, silicate melt, salt melt, experiment, ore genesis*

The problem of liquid immiscibility in natural endogenous processes was studied by many prominent scientists in petrology (F.Yu. Levinson-Lessing, A.A. Marakushev, D.S. Korzhinskiy, V.A. Zharikov, E. Roedder, etc.). To date, an extensive petrological and geochemical material has been accumulated, which indicates phase heterogeneity of natural melts and solutions. However, the question of the connection of this heterogeneity with the processes of magmatism and ore formation remains relevant. Works for example (Marakushev, 1979; Marakushev et al., 1983; Gramenitskiy, 1986) are devoted to solving this problem.

According to numerous experimental data, magmas are concentrators of ore metals with respect to equilibrium with them aqueous fluids of the most diverse composition. The data on the study of the limiting solubility of a number of ore components (REE, Nb, Ti) in silicate melts indicate their low content, depending on the melt composition, as a rule, not exceeding the first percentages (Borodulin et al., 2009; Chevychelov et al., 2010 ; Suk, Kotelnikov, 2008, Suk et al., 2013). These contents are not enough to form rich deposits by direct crystallization from the melt. Liquid immiscibility makes it possible to explain the mechanism of ore substance concentration in the magmatic process from initially low to industrial concentration.

Previously, liquid immiscibility was identified by numerous experimental studies in systems of various types. The article presents the results of experimental studies of phase relations and distribution of elements in the systems silicate melt – salt melt, silicate melt I – silicate melt II, as well as in fluid-magmatic systems in the presence of alkali metal fluorides.

The experiments were carried out on a high gas pressure vessel and on hydrothermal installations with external heating and a cold shutter in sealed platinum and gold ampoules, where the hitch was placed and, if necessary, water was poured. The duration of the experiments ranged from several hours to 1 day, then isobaric quenching was carried out.

The compositions of the obtained samples were determined by electron probe X-ray spectral analysis (EZSRA) using the following instruments (IEM RAS): Camebax x-ray microanalyzer (Cameca, France) with an Link AN-10000 energy dispersive spectrometer (Oxford Instruments, England); Tescan Vega TS5130MM scanning electron microscope (Tescan, Czech Republic) equipped with INCA Energy 200 X-ray microanalysis system with Link INCA Energy energy dispersive spectrometer (Oxford Instruments, England); Tescan Vega II XMU scanning electron microscope (Tescan, Czech Republic) equipped with an INCA Energy 450 X-ray microanalysis system with energy dispersive (INCAx-sight) and crystal diffraction (INCA wave 700) X-ray spectrometers (Oxford Instruments, England) and software platform INCA Energy+.

SILICATE-SALT SYSTEMS. Liquid immiscibility in various silicate-salt systems (with the participation of carbonates, phosphates, fluorides, chlorides, sulfates) was investigated.

Silicate-fluoride systems. Silicate-fluoride liquid immiscibility was obtained in various systems: granite melt – fluoride melt of different composition (defined by K_2SiF_6, Na_2SiF_6, $CaSiF_6$, NaF, CaF_2, LiF in various combinations) at 960°C and 1 kbar (Marakushev, Shapovalov, 1994). aluminosilicate (granite) melt – fluoride salt melt at 800, 900 and 1200°C and 1–2 kbar (Fig. 1) (Kotelnikov et al., 2019a); as well as in the melting of trachyryolites of Central Mongolia (at T=1250°C and P=5.5 kbar), anomalously enriched in CaO and F to 15–20 and 10–15 wt.%, respectively (Suk et al., 2017).

The study of the interphase distribution of ore elements makes it possible to state that fluoride extraction in granite systems is extremely effective as a factor in the concentration of ore matter capable of forming ore deposits. A fundamental separation of ore metals is established by their ability to salt extraction in the studied granite-fluoride systems. Fluoride melts are efficiently extracted tungsten, molybdenum and lead, as well as lanthanum and, to a lesser extent, other rare-earth elements from granite magmas. In contrast to these elements, niobium, tantalum and tin are indifferent to fluoride ore extraction, they remain in granite melts. Zinc is intermediate. Conducted research lays the foundations for metallogenic systematics of ore metals in relation to fluoride salt extraction.

Silicate-phosphate systems. In the systems studied at T=1250°C and P=2 kbar, liquid immiscibility between silicate and alkali-phosphate melts is established. As a result, there is a separation of elements between the phases, so that Ca, Mg, and Na are concentrated in the phosphate melt. High efficiency of phosphate extraction against REE, Ti, Nb, Ta, W, Sn is revealed. The partition coefficients ($K=C^{phosph.}/C^{sil.}$) for REE are always much more than one, for: Ti are 2–3.4, Nb – from 4 and above, Ta – 1.8–3.1, Sn – 1.36–4.63 (Suk, 1997, 2017). The character of the distribution of Zr between immiscible melts depends on the initial composition of the system, which correlates with the compositions of the resulting immiscible phases. The partition coefficients ($K_{Zr}=C_{Zr}^{phosph.}/C_{Zr}^{SIL.}$) vary from 2.15 to 0.76, decreasing with increasing Ca/(Na+K) and Ca/(Si+Al) ratios and increasing agpaiticity ((Na+K)/Al) of silicate melt .

Silicate chloride systems. The experiments were carried out at 960°C and 1 kbar, as well as at 1200 and 1250°C and 2 kbar. In the experiments, the separation of the initial melts into two liquids, silicate and salt (chloride), was systematically observed.

It has been established that in the chloride system only silicon and aluminum have partition coefficients less than unity, and all other rock-forming metals (Mg, Ca, Na, K, Fe) of granites are distributed predominantly in the chloride phase.

Experiments show that chloride extraction of metals, like any other salt extraction, is selective. Ti, Zr, REE, Nb and Ta are practically not extracted from aluminosilicate melts by chloride melts. However, at 1200°C and 2 kbar, high efficiency of chloride extraction is observed with respect to tungsten, so that it almost completely passes into the chloride melt (Suk, 1997).

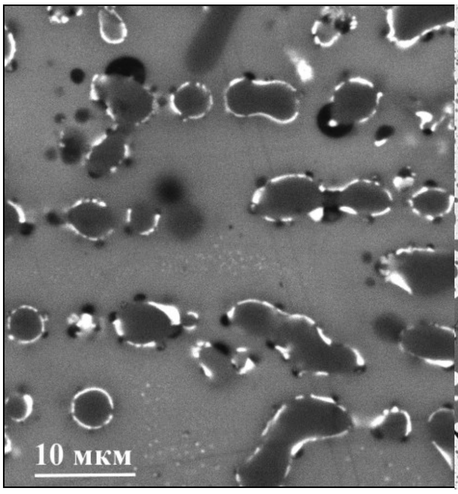

Fig. 1. Separation of fluoride melt in an aluminosilicate matrix in the system of granite melt – sodium fluoride (T=1200°C, P=2 kbar).

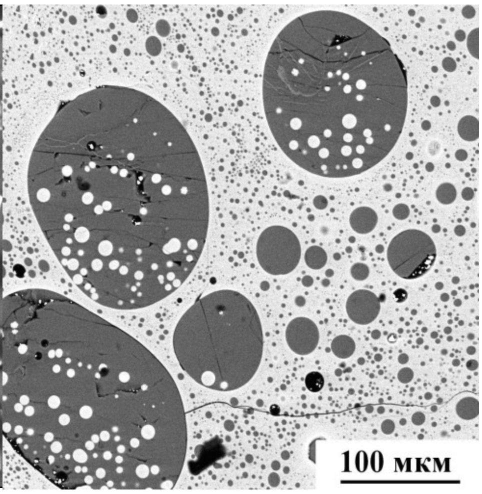

Fig. 2. Liquid immiscibility of silicate-carbonate melts (T=1100°C and P=2 kbar).

Silicate-carbonate systems. An experimental study at T=1100 and 1250°C and P=2 kbar revealed a wide area of layering of silicate-carbonate melts into silicate and carbonate liquids (Fig. 2). The heterogeneity of carbonate liquids is observed, which is manifested in the separation of the carbonate phase into predominantly sodium and alkali-lime fractions. The study of the distribution of REE between silicate and carbonate melts showed that their partition coefficients depend on the initial composition of the system and correlate with the composition of silicate melt (Suk, 2001, 2017). An increase in K_{REE} with an increase in the ratio (Al+Si)/(Na+K+Ca) and with a decrease in the ratio Ca/(Na+K) and Ca/(Si+Al) in a silicate melt is observed. At 1100°C and 2 kbar in alkaline silicate-carbonate systems (where Ca/(Na+K)<0.5 and Ca/(Si+Al)<0.25 in silicate melt), light REE (La, Ce) accumulates in carbonate phases ($K=C_{REE}^{carb.}/C_{REE}^{Sil}.>1$). REEs are predominantly concentrated in the calcium varieties of carbonate melts, while the sodium melts contain almost no REEs. In limestone silicate-carbonate systems (where Ca/(Na+K)>0.5 and Ca/(Si+Al)>0.25 in silicate melt) REE are concentrated in silicate melt. For Y (which is considered as a model of heavy rare-earth elements), the partition coefficients become greater than unity only in systems where Ca/(Na+K) is lower than ~ 0.05, and Ca/(Si+Al) is lower than ~ 0.03.

The inverse dependence of the rare earths partition coefficient on temperature is revealed: with close initial compositions of the systems, its increase from 1100 to 1250°C leads to the redistribution of REE in favor of the silicate phase. This is consistent with the data of D.L. Hamilton et al. (Hamilton et al., 1989). Nb and Ta in the studied systems are concentrated in silicate melt, and Ba and Sr accumulate in carbonate phases.

ALKALINE ALUMINOSILICATE SYSTEMS WITH ORE COMPONENTS. The experiments were carried out in aluminosilicate alkaline systems (composition $Ab_{60}Ne_{40}$) containing Ti, REE (La, Ce), Y, Sr and Nb at 1200 and 1250°C and 2 kbar without the participation of volatile components and under the pressure of water or alkaline water-salt fluids.

In dry systems, the formation of loparite crystals in the silicate matrix was observed. In the same systems, under the pressure of the fluid, melt separation into an aluminosilicate liquid forming a matrix and liquid rich in Ti, REE (La, Ce), Y, Sr and Nb with an admixture of the silicate component forming droplets of 1 to 3 μm has been obtained (Suk, 2012, 2017). The melt in the drops is sharply enriched with Ti, REE and Nb and is depleted of Si and Al. For TiO_2, the partition coefficients ($K=C_{drops}./C_{sil.}$) are greater than 5, for SiO_2 – less than 0.35, for Nb_2O_5 are approximately 10–20, and for REE – more than 15. For SrO, the partition coefficients vary from 2.3 to 7.6.

The titanate-silicate layering was also found during the melting of malignite (the rock with which the richest loparite ores are associated in the Lovozerskiy massif) at 1250°C and 3 kbar in the presence of 15 wt.% H_2O. After the experiment, silicate glass was obtained, in which areas with a microemulsion structure were observed (Fig. 3), as well as rounded ore melt precipitates.

LIQUID IMMISCIBILITY IN ALUMINOSILICATE SYSTEMS. An experimental study of heterogenization in fluid-magmatic systems was carried out on the assumption that two acid silicate melts could coexist, the main difference in which was the water content (Kotelnikov et al., 2017, 2019). Trachyrhyolite (SK-325-5, Yanev, 2003) with composition (wt.%): Na_2O –2.97, MgO – 0.15, Al_2O_3 – 11.51, SiO_2 – 72.78, K_2O – 5.53, CaO – 1.05, TiO_2 – 0.13, FeO – 0.80, SrO – 0.60 was used as the starting material.

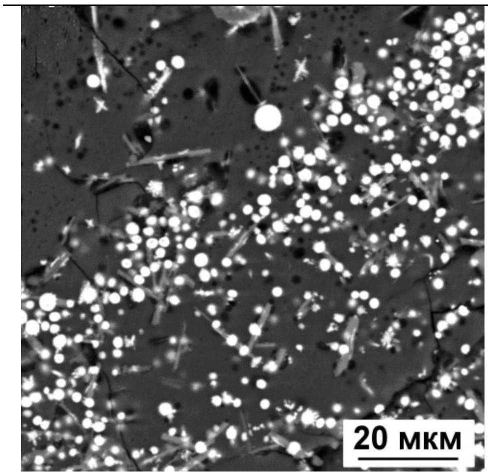

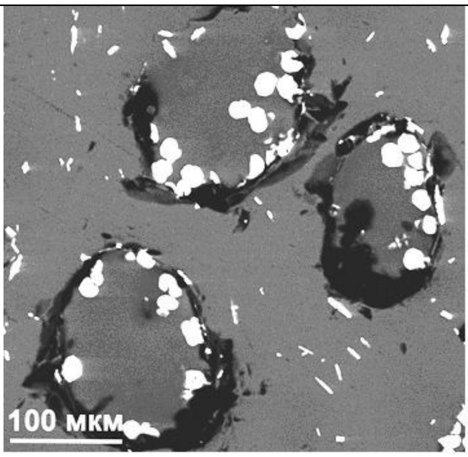

Fig. 3. Liquid immiscibility, obtained by malignite melting at T=1250°C and P=3 kbar in the presence of 15 wt.% H_2O.

Fig. 4. Liquid immiscibility in the experiments of trachyrhyolite melting with additions of La, Nb, Sr (1200°C and 5 kbar → 1000°C and 1 kbar).

The experiments were carried out under special conditions simulating a volcanic process, i.e. with decreasing temperature and pressure characteristic of the process of magma lifting and eruption (1200°C and 5 kbar → 1000°C and 1 kbar) in the presence of 14–15 wt.% H_2O. At 1200°C and 5 kbar, melting, homogenization, and saturation of the melt with fluid components took place. With a decrease in parameters to 1000°C and 1 kbar, liquid immiscibility arose with the formation of droplets (phase L_2) 100–120 μm in size in the melt (phase L_1) (Kotelnikov et al., 2017, 2019b). The distribution of various groups of small (“indicator”) elements (La, Nb, Sr, Rb, Cs, Cr, Fe, Mo, W) between phases L_1 and L_2 was studied.

In the presence of La and Nb droplets (L_2) include isometric crystals of lanthanum niobates (Fig. 4) with the composition $(Ca_{0.08}Fe_{0.16}La_{1.08})_{1.36}(Ti_{0.11}Nb_{0.75})_{0.86}O_4$. In the matrix ($L_1$) there are elongated crystals of the composition $LaNbO_4$. The glass of the L_2 phase is enriched in lanthanum and niobium compared to the L_1 phase. The partition coefficients between these phases, taking into account the total content of lanthanum and niobium (including crystalline phases) in melts L_1 and L_2, are for $Nb_2O_5 \approx 10$ and for $La_2O_3 \approx 29$. At the same time, there is a predominant concentration of lanthanum in L_2 relative to niobium. Experiments have revealed the enrichment of the droplets phase of K, Fe, Rb and Cs (the partition coefficients for the oxides of these elements are 1.26, 2.01, 1.97, and 2.15, respectively). The study of the distribution of Fe and Cr showed that the partition coefficients of Fe (in terms of FeO) and Cr (in terms of Cr_2O_3) are 4.25 and 7.43, respectively, i.e. these elements enrich L_2.

The composition of ore phase crystals corresponds to chromite $(Mg_{0.02}Mn_{0.03}Fe_{0.95})_{1.00}(Al_{0.09}Fe_{0.31}Cr_{1.60})_{2.00}O_4$. Experiments with the addition of $Na_2MoO_4 \times 2H_2O$ and $Na_2WO_4 \times 2H_2O$ salts showed that Mo and W enrich the L_2 drops, whose partition coefficients in terms of MoO_3 and WO_3 are 1.11 and 1.20, respectively. The ore phase is defined as molybdoscheelite $Ca_{1.01}(Mo_{0.33}W_{0.66})_{0.99}O_4$. Its crystals are present both in the matrix (L_1) and in L_2, where there are relatively more of them. Thus, it was established that the composition of the droplets is similar to that of the matrix, differing only in the water content, concentration of the indicator components, and the ratios of alkaline and alkaline-earth elements.

FLUID-MAGMATIC SYSTEMS.To explain the genesis of rare-metal tantalum deposits, the interaction of fluoride solutions (LiF, NaF, KF) with ore-silicate systems (Qz ± granite ± Tnt ± Pchl) was investigated. It was shown that at a temperature of 550 – 850°C and a pressure of ≤1 kbar in the conditions of the existence of a stratified fluid, aluminosilicate (silicate) alkaline glass is formed – low-temperature melt (Kotelnikov et al., 2018), which can contain up to 17 wt.% alkaline oxides (Na_2O+K_2O). Such a low-temperature, high alkaline ($K_{agp} \sim 2$) melt is a concentrator of tantalum and niobium. The content of Nb_2O_5 in glass is up to 8 wt.% (650°C) and up to 6 wt.% (850°C). The concentration of Ta_2O_5 (in experiments with tantalite) in glass reaches 2.6 wt.% (750°C) and 6.1 (850°C). This alkaline low-temperature melt contains up to ~ 10 wt.% volatile components ($F+H_2O$) and can serve as a phase – concentrator of rare-metal elements (Ta, Nb) at the latest stages of crystallization of lithium-fluoride granites of potassium specialization. Due to the concentration of rare metals in this phase, ore accumulations of tantalum and niobium minerals are formed in the upper parts of the massifs of lithium-fluoride granites – the so-called apogranites (Beus et al., 1962).

CONCLUSIONS

1. Experimental foundations were laid for the construction of geochemical models of the behavior of elements in liquid immiscibility processes.

2. The conclusion is made about the leading role of liquid immiscibility processes for the concentration of ore elements and the formation of mineral deposits at the magmatic stage.

3. Experimental data are presented for studying the salt extraction of a number of ore elements (Y, REE, Sr, Ba, Ti, Nb, Ta, Mo, W, Pb) in silicate-salt systems at a temperature of 850-1250°C and a

pressure of 1-5.5 kbar. It is shown that the interphase partition coefficient is sufficient for the formation of ore deposits.

4. The processes of liquid immiscibility in a fluid-saturated melt of trachyryolite were studied. Its separation into two silicate liquids is shown, and the interphase partition coefficients of a series of elements (Sr, La, Nb, Fe, Cr, Mo, W, K, Rb, Cs) are determined.

5. The processes of interaction of heterophase fluid in the granite (quartz) – ore mineral – heterophase fluid system (Li, Na, K-fluoride) at 650–850°C and 1 kbar were studied. The formation of a highly alkaline fluid-saturated silicate melt, which is a Ta and Nb concentrator, as a result of the reaction of the fluid with rock and ore minerals has been demonstrated. This phase is responsible for the concentration of ore components and at the same time is the environment of ore deposition (formation of ore "apogranites" and quartz veins).

References:

Beus A.A., Severov E.A., Sitnin F.F., Subbotin K.D. Albitized and greisenized granites (apogranites). M. USSR Academy of Sciences. 1962. 196 p.

Borodulin G.P., Chevychelov V.Y., Zaraysky G.P. Experimental study of partitioning of tantalum, niobium, manganese, and fluorine between aqueous fluoride fluid and granitic and alkaline melts. Doklady Earth Sciences. 2009. V. 427. N 1. P. 868-873.

Gramenitskiy E.N. To the knowledge of the evolution of hydrothermal-magmatic systems. Vestnik Mosk. University. Ser. geology. 1986. N. 2. P. 3–17.

Kotelnikov A. R., Suk N. I., Kotelnikova Z. A., Yanev Y., Encheva S., Ananiev V. V. The study of liquid immiscibility in fluid-magmatic systems. "Proceedings of the All-Russian Annual Workshop on Experimental Mineralogy, Petrology and Geochemistry. Moscow, April 18–19, 2017". M: VIGAC RAS. 2017. P. 64–67.

Kotelnikov A. R., Korzhinskaya V.S., Kotelnikova Z. A., Suk N. I., Shapovalov Yu.B. Solubility of tantalite and pyrochlore in fluoride solutions at T=650-850°C and P=1 kbar in the presence of silicate substance. "Proceedings of the All-Russian Annual Workshop on Experimental Mineralogy, Petrology and Geochemistry. Moscow, April 18-19, 2018. " M: VIGAC RAS. 2018. P. 160-163.

Kotelnikov A. R., Suk N. I., Korzhinskaya V. S., Kotelnikova Z. A., Shapovalov Yu. B. Phase Distribution of Rare and Rare-Earth Elements in the Silicate–Fluoride Systems at T = 800–1200°C and P = 1–2 kbar (Experimental Investigations). Doklady Earth Sciences. 2019a. V. 484. N 2. 185-188.

Kotelnikov A. R., Suk N. I., Kotelnikova Z. A., Yanev Y., Encheva S., Ananiev V. V. Liquid Immiscibility in Fluid–Magmatic Systems: An Experimental Study. Petrology. 2019b. V. 27. N. 2. P. 186–201.

Marakushev A.A. Petrogenesis and ore formation (geochemical aspects). M .: Nauka. 1979. 262 p.

Marakushev A.A., Gramenitskiy E.N., Korotaev M.Yu. Petrological model of endogenous ore formation. Geology of ore deposits. 1983. № 1. P. 3–20.

Marakushev, A.A., Shapovalov, Yu.B. Experimental study of ore concentration in fluoride granite systems. Petrology. 1994. V. 2. N. 1. P. 4–23.

Marakushev, A.A., Shapovalov, Yu.B. Behavior of molybdenum, lead and zinc in fluoride salt extraction processes. Doklady Earth Sciences. 1996. V. 351. N. 5. P. 670–672.

Suk N.I. Behavior of ore elements (W, Sn, Ti and Zr) in layering silicate-salt systems. Petrology. 1997. V. 5. N 1. P. 20-27.

Suk N.I. Experimental study of liquid immiscibility in silicate-carbonate systems. Petrology. 2001. V. 9. N 5. P. 477-487.

Suk N.I. Experimental study of liquid immiscibility in the fluid-magmatic silicate systems containing Ti, Nb, Sr, REE, and Zr. Petrology. 2012. V. 20. N 2. P. 138-146.

Suk N.I. Liquid immiscibility in alkaline magmatics systems. 2017. M.: "KDU", "University Book". 238 p.

Suk N. I., Kotelnikov A. R. Experimental study of loparite formation in complex fluid-magmatic systems. Doklady Earth Sciences. 2008. V. 419. N 2. P. 463-466.

Suk N. I., Kotelnikov A. R., Viryus A.A. Crystallization of loparite in alkaline fluid-magmatic systems (from experimental and mineralogical data). Russian Geology and Geophysics. 2013. V. 54. N 4. P. 436-453.

Suk N. I., Kotelnikov A. R., Peretyazhko I.S., Savina E.A. An experimental study of the melting of trachyryolites of Central Mongolia. "Proceedings of the All-Russian Annual Workshop on Experimental Mineralogy, Petrology and Geochemistry. Moscow, April 18–19, 2017". M: VIGAC RAS. 2017. P. 80-83.

Hamilton D.L., Bedson P., Esson J. The behaviour of trace elements in the evolution of carbonatites. In "Carbonatites. Genesis and evolution". Bell K.,Ed., London: Unwyn Hyman, 1989. P. 405-427.

Yanev Y. Petrology of Golobradovo perlite deposit, Eastern Rhodopes. Geochem. Mineral. Petrol. Sofia. 2003. V. 40. P. 1–20.

Kotelnikov A.R.[1], Kotelnikova Z.A.[2], Suk N.I.[1], Gramenitskiy E.N.[3] Problems and tasks of experimental mineralogy and petrology UDC 550.4.02

[1]Institute of Experimental Mineralogy RAS (IEM RAS), Chernogolovka Moscow district, (kotelnik@iem.ac.ru; sukni@iem.ac.ru); [2]Institute of Geology of Ore Deposits, Petrography, Mineralogy, and Geochemistry RAS (IGEM RAS), Moscow (kotelnik@igem.ac.ru); [3]M.V. Lomonosov Moscow State University, Geological Faculty, Moscow (engramen@geol.msu.ru)

Abstract. The active development of experimental methods for the study of mineralogical and petrological problems began in our country about half a century ago. At this time, experimental research centers were established in Leningrad, Kiev, Moscow, Chernogolovka, Novosibirsk, Irkutsk, Yakutsk, and Vladivostok. Tasks to study the properties of fluids, melts, fluid-magmatic systems, the properties of solid solutions of minerals, etc. were successfully solved. Metasomatism, metamorphism and hydrothermal equilibria of mineral parageneses were simulated. Much attention was paid to hydrothermal processes – the study of the transport of ore matter, crystal growth, simulation of equilibria in the mineral-water solution systems. To date, we have come to new frontiers in the study of matter and endogenous processes. Therefore, we would like to formulate new perspective problems and tasks. The presentation should be divided into subsections: (1) scientific problems (2) applied (3) methodical (4) technical tasks. The report presents our view on the ways and methods of development of experimental petrology.

Keywords: *experimental mineralogy and petrology, fluid-magmatic systems, melts, mineral paragenesis, hydrothermal processes, metamorphism, metasomatism*

The active development of experimental methods for the study of mineralogical and petrological problems began in our country about half a century ago. At this time, experimental research centers were established in Leningrad, Kiev, Moscow, Chernogolovka, Novosibirsk, Irkutsk, Yakutsk, and Vladivostok. The tasks of studying the properties of fluids, melts, fluid-magmatic systems, the properties of solid solutions of minerals, etc. were successfully solved. Our leading scientists, starting with academician A.P. Vinogradov, (D.S. Korzhinskiy, A.A. Marakushev, V.A. Zharikov, I.D. Ryabchikov, L. L. Perchuk, etc.) laid the theoretical foundations of physics-chemical petrology and geochemistry. Experimental studies were initiated by works on the industrial synthesis of piezoelectric crystals (including quartz), as well as the creation of a special laboratory of experimental research under the supervision of N.I. Khitarov (A.A. Kadik, E.B. Lebedev, S.D. Malinin, E.E. Senderov).

Much attention was paid to the properties of aluminosilicate melts: their rheological properties, solubility in them of volatile components and much more were studied. The objectives of these studies were to solve petrological problems: determining the RT parameters of the existence of igneous melts and other phases associated with them; reasons for the diversity of compositions of eruptive rocks; mechanisms of magma differentiation; regularities of evolution of magma compositions with their differentiation; magma formation mechanisms; interaction of igneous melts with host rocks; connection magmatism with hydrothermal processes and ore genesis. In addition, the processes of metasomatism, metamorphism and hydrothermal equilibria of mineral parageneses were modeled. Much attention was paid to hydrothermal processes — studies of phase diagrams of the systems that are most important for petrology, ore transport, crystal growth, modeling equilibria in mineral — water solution systems.

At the turn of the century, science in our country and abroad experienced a systemic crisis associated with the reduction of funding and the closure of many research centers. Nevertheless, research continued and so far we have come to new frontiers in the study of matter and endogenous processes. Therefore, we would like to formulate new perspective problems and tasks.

We confine ourselves only to the processes in the Earth's crust. The mass of the earth's crust is only half a percent of the mass of the entire planet, but its diversity and variety of processes occurring in it are extremely large. Most of the ore-generating igneous melts formed within the depths of the middle and lower crust. And the greatest variety of ore-forming processes is associated, as a rule, with relatively low RT parameters. Therefore, processes in the crust are of exceptional interest for experimental studies.

1. Problems of magmatism.

The origin of magmatic melts is associated with the processes of deep anatexis, palingenesis and the formation of melts under the influence of fluids that change their composition (metasomatism). These processes are associated with large collisions caused by mantle processes. The opening of deep faults is accompanied by the formation of igneous melts during the interaction of a lower crust substrate with fluid components. In the course of the evolution of deep-seated magmatic melts in the presence (or absence) of fluid with a decrease in the TP parameters, heterogenization of the initially homogeneous melt occurs. In the process of heterogenization, the aqueous phase enriched in the salt component is separated from the melt (such salts can be sulfides, carbonates, phosphates, chlorides, sulfates and chlorides). With certain compositions of the melt, heterogenization of the aluminosilicate melt can occur into two phases differing in different volatile content (Zharikov, 2005; Kotelnikov et al., 2019). All these processes occur when the pressure decreases from ~ 10-12 kbar (lower crust) to 1-3 kbar and the temperature decreases from ~ 1200°C to 800-900°C. The process of separation of volatile also proceeds with a decrease in PT parameters. It should be noted that the processes of occurrence of immiscibility are not a one-act process, but are complex, multistage in nature. Such behavior is characteristic of PQ-type systems, which include fluid-magmatic systems. The evolution of heterogeneous magmatic systems is accompanied by the redistribution of elements (both petrogenic and ore) between the coexisting phases associated with the processes of acid-base interaction. In this case, the aluminosilicate melt can increase the alkalinity (Zharikov, 1987). Thus, the composition of the original igneous melt changes. With an increase in alkalinity, the aluminosilicate melt begins to actively extract ore elements from host rocks. At the same time, in the complex heterophase system (melt - vapor - saline liquid), the ore elements are redistributed into the salt phase, also. During the crystallization of such silicate melts and their associated salt melts, complexes of alkaline magmatic rocks are formed, enriched in rare elements. All these massifs are distinguished by deep genesis and complex evolution during the formation of crystalline rocks. They are confined to the deep faults of the shields of ancient rocks, along which the magma saturated with fluid components moved. For granite melts, we have shown the possibility of the formation of high-alkaline solution-melts in the later stages of the crystallization of lithium fluoride granites. This phase is formed due to the interaction of heterophase fluid of (Li,Na,K)F composition at low pressures with crystalline (or melt-crystalline) phases of lithium-fluoride granites. Such a highly alkaline melt concentrates rare elements (Ta, Nb) and can be responsible for the formation of deposits of these metals.

At the same time, the following problems remain experimentally insufficiently solved:

– the origin of primary melts and their subsequent evolution;

– fluid-magmatic interaction during the rise of magmatic melts;

– interaction with host rocks – contamination of the substance;

– determination of analytical dependences of solubility of volatile (H_2O, CO_2) and salt components in magmatic melts in a wide range of TPX parameters.

It is advisable to solve such problems on apparatus such as gas bombs in ampoule volumes sufficient for fluid extraction. In addition, these apparatus allow you to smoothly change the PT-parameters of the experiments in a wide range of temperatures and pressures. The operating parameters of such an installation should be as follows: P=10-0.2 kbar; T=1250-700°C. Methods of local analysis are also needed for low concentrations of elements (100-1000 ppm) with locality ~ 1-3 µm (!).

2. Experimental study of minerals and their solid solutions

Here, in our opinion, the main research should be focused on the study of minerals and their associations in order to: a detailed study of their properties for use in the numerical simulation of petrogenesis processes; development of geothermometer complexes covering the entire spectrum of the existing rocks with parameters of petrogenesis of the earth's crust (P=10-0.2 kbar; T=1250 - 200°C). Now there are software systems such as Komagmat, Petrologist, allowing to simulate the crystallization of the basic melts. In addition, there are K. Putyrka semi-empirical programs for estimating the parameters of the formation of basaltic complexes by mineral-melt equilibria. For metamorphic rocks, the TWQ and Selector software complexes are successfully used, which make it possible to simulate metamorphic rocks parageneses well enough and solve the inverse problem — estimating the TP parameters of mineralogenesis from mineral paragenesis. At the same time, there are problems in estimating the temperatures of petrogenesis of igneous complexes of medium and acidic composition, alkaline and highly alkaline rocks.

Unresolved tasks.

1. The study of the thermodynamic properties of solid solutions of minerals, both rock-forming and accessory. This is necessary for the development of numerical modeling and the construction of geothermometers and geobarometers. Practically there are no data on solid solutions of amphiboles.

2. The study of mineral equilibria with the participation of ternary solid solutions (now partially studied the equilibrium of nepheline with different contents of the albite molecule, as well as feldspar). Polycomponent solid solutions of amphiboles, clino- and orthopyroxenes, biotites, garnets, etc. remain practically unexplored.

3. Correlation of methods of isotope thermometry with data on temperature estimation by methods of mineral thermometry.

4. Experimental study of the structural ordering of minerals and their solid solutions, depending on the TPX parameters.

3. Fluid systems.

Over the past half century, the study of the fluid phase has yielded very interesting results. Phase diagrams of the most important for the processes of petro- and mineragenesis of fluid systems, such as: $H_2O + CO_2$; $H_2O + NaCl$; $H_2O + KCl$; $H_2O + NaCl + CO_2$ are produced.

The PVT properties of gases and their mixtures are experimentally studied to high PT parameters. Methods for assessing the fluid state at high parameters have been developed – the study of synthetic fluid inclusions, new analytical methods for determining the qualitative and quantitative characteristics of the fluid (Raman spectroscopy, laser ablation and mass spectrometry, etc.). The most important role of fluids in the processes of petrogenesis and ore matter transport is shown. By now, we can, knowing the behavior of fluids in systems of the first and second types, begin experimental modeling of fluid-magmatic interaction. That is, we can investigate the distribution of elements in fluid-magmatic systems with the participation of heterogeneous phases, both fluid and melt. As preliminary experiments have already shown, in such systems it is necessary to take into account the processes of high-temperature hydrolysis and the interphase separation of acid and alkaline components. In this case, concentrated salt fluids enriched in alkalis (heavy fluid) and the vapor phase enriched in acidic components can form. The distribution of ore elements between the “heavy fluid” and the acid phase and their transport by these phases can explain a number of features of the ore genesis process.

Unsolved problems

1. The lack of computational methods for modeling complex systems involving silicate substances and active saline fluid. Apparently, experimental studies are needed here to estimate the activities of the components in complex solutions.
2. The existing experimental methods do not allow sampling phases of solutions at high parameters (above 600°C and P> 2 kbar).
3. We need new local methods for studying the composition of the phases of fluid inclusions.

References:

Zharikov V.A. Fundamentals of physical geochemistry. M .: Izd. MSU. 2005. 654 p,

Kotelnikov A. R., Suk N. I., Kotelnikova Z. A., Yanev Y., Encheva S., Ananiev V. V. Liquid Immiscibility in Fluid–Magmatic Systems: An Experimental Study. Petrology. 2019. V. 27. N. 2. P. 186–201.

Persikov E.S., Bukhtiyarov P.G., Nekrasov A.N., Shaposhnikova, O. Y. .The effect of H_2O on the chemical interdiffusion of major components (SiO_2, Al_2O_3, Na_2O, CaO, MgO) in andesite - basalt system

Institute of Experimental Mineralogy, Russian Academy of Sciences. Chernogolovka. persikov@iem.ac.ru

Abstract. Continuation of our early works this paper presents the results of experimental and theoretical studies of the effect of water dissolved in melts on the chemical interdiffusion of petrogenic components (SiO_2, Al_2O_3, Na_2O, CaO, MgO) in the interaction of model melts of the andesite-basalt system. The rates of chemical interdiffusion of all petrogenic components (SiO_2, Al_2O_3, Na_2O, CaO, MgO) are almost identical in the interaction of anhydrous andesite and basalt melts. This type of diffusion is maintained at a concentration of water dissolved in the melts, up to ~ 2 wt. %. This behavior may indicate that inter-diffusion of equal velocities of molecules of albite and diopside in opposite directions in the interaction of anhydrous andesitic and basaltic melts. With an increase in the concentration of water dissolved in these melts, the diffusion mechanism changes dramatically, since all petrogenic components diffuse at different rates, indicating a significant depolymerization of the melts. Theoretical analysis of the data on the chemical interdiffusion of petrogenic components, as well as water diffusivity in melts in the andesite-basalt series, and their viscosity, allowed established a natural relationship between the two important transport properties of magmas.

Keywords: *H_2O, chemical diffusion, components, andesite-basalt, temperature, pressure, viscosity*

Studies of the effect of dissolved H_2O on the chemical interdiffusion of petrogenic components in the interaction of magmatic melts are extremely limited (Chekhmir et al., 1991; Watson and Baker, 1991; Watson, 1994; Yoder, 1973; Baker, 1991; Persikov et al., 2011). The majority of published work on the diffusion of major components in magmatic melts and the influence of dissolved water on the speeds of chemical diffusion is performed by dissolution of minerals (Chekhmir et al., 1991; Watson and Baker, 1991; etc.). While studies of the interdiffusion of these components directly in melts are extremely limited (Yoder, 1973; Watson and Baker, 1991). Along with preliminary data (Persikov et al., 2011), this paper presents the results of experimental and theoretical studies of the effect of water dissolved in melts on the chemical interdiffusion of petrogenic components (SiO_2, Al_2O_3, Na_2O, CaO, MgO) in the interaction of model melts of the andesite-basalt system. The studies were carried out using the original apparatus of high gas pressure at water pressures up to 200 MPa, argon pressures up to 200 MPa and temperature T = 1300 ^oC, using the method of diffusion pairs (Persikov, Bukhtiyarov, 2002). Two types of diffusion pairs were used in experiments. Run durations are 480 - 1500 s. 1. Anhydrous model glasses of andesite (Ab75Di25, mol. %) and basalt (Ab50Di50, mol.%) compositions were introduced into contact and melted in welded platinum ampoules at P(Ar) up to 200 MPa; 2. The same glasses with the different content of dissolved water in pairs (1.0, 2.1, 4.3, and 5.6 wt. %), were also introduced into contact and melted in welded platinum ampoules at P(Ar) up to 200 MPa. The necessary anhydrous and water-containing glasses of model andesite and basalt compositions were synthesized using the same high gas pressure apparatus at a temperature of 1300 ^oC, argon pressures (anhydrous glasses) and water vapor pressures (water-containing glasses) up to 200 MPa.

The water content in water-bearing samples and along diffusion profiles was determined by quantitative micro-IR spectroscopy (Persikov et al., 2010; Persikov et al., 2010), and the distribution of petrogenic components along diffusion profiles were measured on a microprobe (see fig. 1). The coefficients of chemical interdiffusion of petrogenic components (SiO_2, Al_2O_3, Na_2O, CaO, MgO) in the studied melts are determined by numerical solution of the diffusion equations using the Gauss error function (Crank, 1975). The results on the effect of dissolved water on the chemical interdiffusion mobility of petrogenic components are presented in the table and in figure 2.

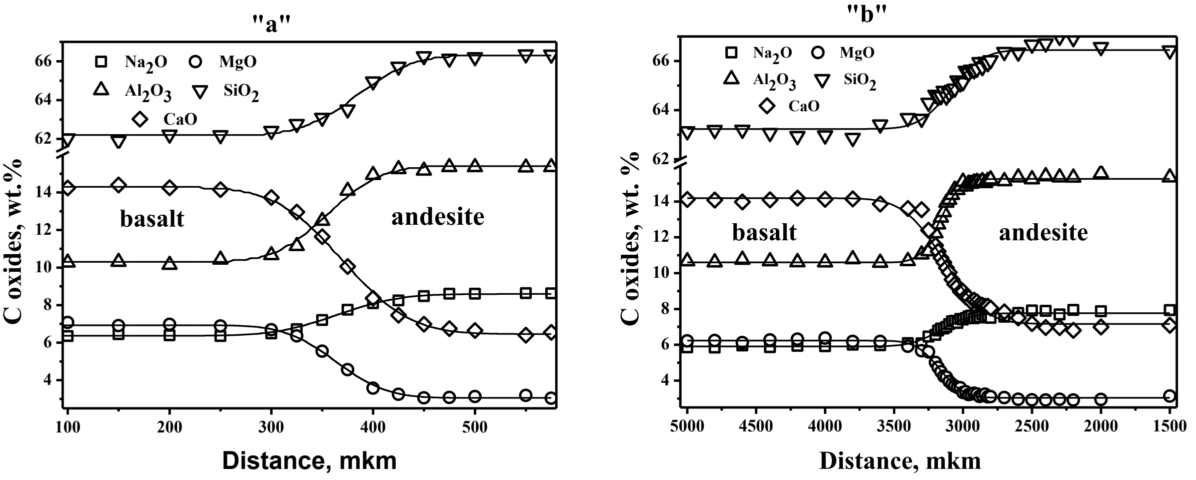

Fig.1. Measured concentration profiles of major components in the system basalt – andesite - water at the T = 1300°C and at the Ar pressures up to 100 MPa (the curves at the all diagrams are error function fits, Crank, 1975).
a – water free melts, run No 1641/1, run duration was 480 s; b - water bearing melts, run No 1650/4, run duration was 1320 s, water content was 4.3 wt. % (Persikov et al., 2011).

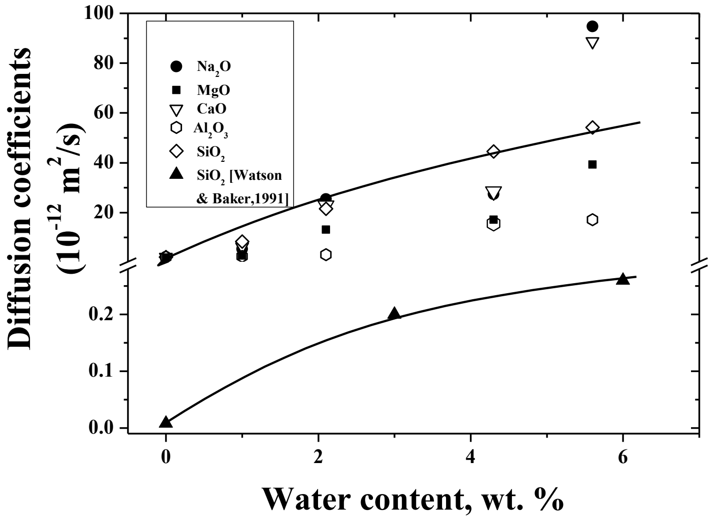

Fig.2. Dependences of chemical interdiffusion coefficients of petrogenic components (SiO_2, Al_2O_3, Na_2O, CaO, MgO) on water concentration in the melts at interaction of model basalt and andesite melts (T = 1300 °C, water pressure up to 200 MPa), in comparison with similar dependence for SiO_2 from (Watson and Baker, 1991; Baker, 1991) at interaction of dacite-rhyolite melts. (T = 1300 °C, at 1 GPa total pressure and water pressure up to 200 MPa).

Table. The coefficients of the chemical interdiffusion of major components and end-members of minerals in the model melts of andesite-basalt-water system (the experiments were performed at T = 1300 °C and a pressure up to 200 MPa ($D\cdot10^{-12}$ m^2/s).

Oxydes	1641/1 $X(H_2O) = 0$	641/3 $X(H_2O) = 2.1$ wt. %	1650/4 $X(H_2O) = 4.3$ wt. %	1674/1 $X(H_2O) = 5.6$ wt. %
Na_2O	2.0±0.4	24.0±3.6	26.0±3.8	95.0±5.4
MgO	1.6±0.32	17.0±3.4	19.0±2.2	40.0±4.9
Al_2O_3	1.7±0.34	7.5±1.7	17.0±1.4	18.5±2.1
SiO_2	2.0±0.4	20.2±2.0	41.0±4.3	54.0±4.2
CaO	2.2±0.44	21.4±2.6	28.0±3.6	88.0±4.6
Molecules				
Ab	1.9±0.38	18.8±2.8		
Di	1.87±0.38	20.0±3.0		

Analysis of the experimental data allows us to draw the following conclusions:

1. The rates of chemical interdiffusion of all petrogenic components (SiO_2, Al_2O_3, Na_2O, CaO, MgO) are almost identical in the interaction of anhydrous andesite and basalt melts. In this case, the rate of diffusion of network forming cations (SiO_2, Al_2O_3) is about two orders of magnitude higher compared to their tracer diffusion (Watson, 1994; etc.). On the contrary, the rate of diffusion of the cations-modifiers (Na_2O, CaO, MgO), lower by about one order of magnitude compared to their tracer diffusion (Watson, 1994; etc.). This behavior may indicate a nominal chemical mechanism of

interdiffusion, i.e., interdiffusion of equal velocities of molecules of albite and diopside in opposite directions in the interaction of anhydrous andesitic and basaltic melts. This type of diffusion is maintained at a concentration of water dissolved in the melts, up to ~ 2 wt. % (fig. 2 and table).

2. With an increase in the concentration of water dissolved in these melts, the diffusion mechanism changes dramatically, since all petrogenic components diffuse at different rates, indicating a significant depolymerization of the melts, as a result of the dissolution of water in them (fig. 2 and table). The analogous nature of the established dependence is evident in comparison with the results of the work (Watson and Baker, 1991). The differences in the absolute values of the diffusion coefficients of SiO_2 are easily explained by the different degree of depolymerization and, consequently, by the different viscosity of the melts in the andesite-basalt system (present work) in comparison with the dacite-rhyolite system in the work (Watson and Baker, 1991).

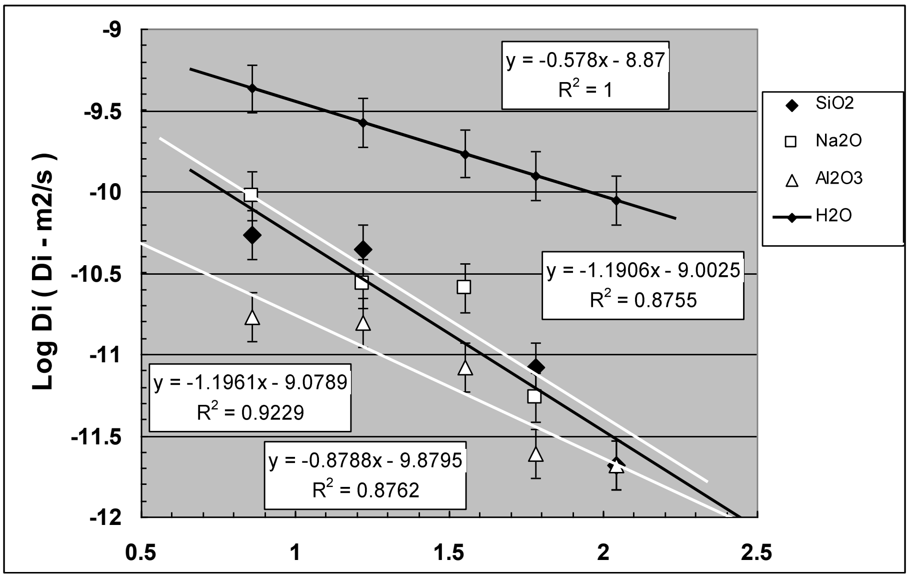

Fig. 3. Relationship between interdiffusivities of a few major components (SiO_2, Al_2O_3, Na_2O), diffusivity of water and melt viscosity over the range of silicate melt compositions from andesite to basalt (water pressures up to 200 MPa, T = 1300 °C and water content into melts up to 5.6 wt. %).

3. The rates of interchemical diffusion of all petrogenic components, with water concentration in andesitic and basalt melts ≥ 2 wt. %, increase by about an order of magnitude compared to anhydrous melts. However, the degree of influence of water dissolved in melts on the chemical interdiffusion coefficients of all petrogenic components decreases significantly with further increase of water concentration in such melts (fig. 2).

On the basis of a new low-gradient methodology, reliable experimental data on the diffusion mobility of water in magmatic melts in the andesite – basalt series in wide ranges of H_2O concentrations (0.1 - 6 wt. %), temperatures (1000° – 1300 °C) and water pressures up to 200 MPa have been obtained (Persikov et al., 2010). Theoretical analysis of the data on the chemical interdiffusion of petrogenic components, as well as water diffusivity in melts in the andesite-basalt series, and their viscosity, allowed to establish a natural relationship between the two important transport properties of magmas (Persikov et al., et al., 2011). This relationship is qualitatively consistent with the Stokes-Einstein law and the Eiring relation on the inversely proportional relationship between the viscosity of the liquid and the diffusion of the components in it (Fig. 3).

Melts viscosity along diffusion profiles was determined with sufficient accuracy using our structural-chemical model of prediction and calculations of viscosity of model and magmatic melts (Persikov, 1998; Persikov and Bukhtiyarov, 2009). As a result, simple dependences D = f(η) for all petrogenic components are obtained, which are recommended for calculations of the diffusion mobility of petrogenic components in the interaction of melts not studied experimentally. Figure 3 shows some examples: $\log D(SiO_2) = -1.2\log\eta - 9.1$; $\log D(Na_2O) = -1.19\log\eta - 9.0$; $\log D(Al_2O_3) = -0.88\log\eta - 9.8$. It is also established that at comparable values of T, P – parameters and melt compositions, the diffusion mobility of H_2O is an order of magnitude higher than the diffusion mobility of all petrogenic components, including alkalis (see fig. 3).

The authors are grateful to S. Newman (Caltech, USA) and G. V. Bondarenko (IEM RAS) for their help in determining the water content in melts (glasses) using IR spectroscopy.

The work was carried out under the theme No 2 (IEM RAS) with the financial support of the program No 19 of the Presidium of RAS.

References:

Baker D. R. (1991). Interdiffusion of hydrous dacitic and rhyolitic melts and the efficacy of rhyolite contamination of dacitic enclaves. Contrib. Miner. Petrol. v. 106, p. 462-473.

Chakraborty, S. (1995). Diffusion in silicate melts. Structure, dynamics and properties of silicate melts. Reviews in Mineralogy. Eds. Stebbins J. F., McMillan P. F. and Dingwell D. B., Miner. Soc. Amer. v. 32, p. 412-503.

Crank J. (1975). The mathematics of diffusion. Oxford. Clarendon Press, 414 p.

Persikov E. S., Bukhtiyarov P. G. (2002). Unique gas high pressure apparatus to study fluid - melts and fluid - solid - melts interaction with any fluid composition at the temperature up to 1400°C and at the pressures up to 5 kbars. J. Conf. Abs., 2002, v. 7, No. 1, p. 4. 85.

Persikov E. S. (1998). Viscosity of model and magmatic melts at T, P – parameters of the earth's crust and upper mantle. Russian Geology and Geophysics. v. 39, No 12, p. 1780-1792.

Persikov E. S., P. G. Bukhtiyarov (2009). Interrelated structural-chemical model to predict and calculate viscosity of magmatic melts and water diffusion in a wide range of compositions and T,P – parameters of the Earth's crust and upper mantle. Russian Geology and Geophysics, v. 50, p. 1079-1090.

Eduard S. Persikov, Sally Newman, G. Bukhtiyarov Pavel, Alexey N. Nekrasov, Edward M. Stolper (2010). Experimental study of water diffusion in haplobasaltic and haploandesitic melts. Chem. Geol., v. 276, p. 241-256.

Persikov E.S., P.G. Bukhtiyarov, A.N. Nekrasov (2010). Water diffusion in basalt and andesite melts under high pressures. Geochemistry International, v. 48, No 3, p. 213-224.

E. S. Persikov, P. G. Bukhtiyarov, A. N. Nekrasov (2011). The relationship between the diffusion of petrogenic (SiO2, Al2O3, Na2O, CaO, MgO, FeO, TiO2) and volatile components (H2O) and the melt viscosity of the obsidian-dacite-andesite-basalt system (experimental and theoretical study). Vestnick AN, v. 3, NZ6076. Doi: 10.2205/2011NZ000206

Shekhmir A. S., Simakin A. G., Epelbaum M. B. (1991). Dynamic phenomena in fluid-magmatic systems. Ed. Zaraiskiy G. P. Nauka: M., 141 p.

Watson E. B., Don R. Baker (1991). Chemical diffusion in magma: An overview of experimental results and geochemical applications. Physical chemistry in magma. Advances in physical geochemistry. Eds. Perchuk L. L., Kushiro, I. Springer-Verlag. v. 9, p. 120-151.

Watson E. B. (1994). Diffusion in volatile-bearing magmas. Volatiles in magmas. Reviews in Mineralogy. Eds. Carrol M. R. and Holloway J. R. Miner. Soc. Amer. v. 30, p. 371-411.

Yoder H. S. (1973). Contemporaneous basaltic and rhyolitic magmas. Am. Mineral. v. 58, p. 153-171.

Rusak A.A.[1], Shchekina T.I.[1], Alfereva Ya. O.[1], Gramenitsky Ye.N.[1], Kotelnikov A.R.[2], Zinovieva N.G.[1], Bychkov A.Yu.[1], Akhmedzhanova G.M.[2] The effect of temperature and pressure on phase relations and the distribution of yttrium, scandium and rare earth elements in granitic system Si-Al-Na-K-Li-F-O-H. UDC 552.11, 550.42.

[1] Lomonosovi Moscow State University, Department of Geology, Russia, Moscow, [2] Institute of Experimental Mineralogy RAS, Russia, Chernogolovka (aleks7975@yandex.ru, t-shchekina@mail.ru; *yanaalf@yandex.ru*, engramen@geol.msu.ru, kotelnik@iem.ac.ru, nzinov@mail.ru, andrewbychkov@rambler.ru, akhm@iem.ac.ru)

The distribution of rare-earth elements, Y and Sc between aluminosilicate (L) and aluminofluoride (LF) melts in a granite system with limiting fluorine concentrations at a temperature of 600, 700 and 800 °C, a pressure of 1 and 2 kbar, and a water content of 0 to 50 wt.% was experimentally studied. It is shown that, starting from 700 °C, 1 kbar, the phase relations in the system change. In globules of fluoride melt saturated with rare elements, crystals of KNa-aluminofluorides are isolated, and when the temperature decreases to 600 °C from the silicate melt, quartz begins to crystallize, which proves the approximation to the solidus of the system while maintaining both immiscible melts. It is shown for the first time that the distribution of REE, Y, Sc between coexisting aluminofluoride (salt) and aluminosilicate melts depends on the pressure.

***Keywords**: granite system; rare earth elements; lithium; separation coefficient; aluminosilicate; aluminofluoride; salt melts; water content; pressure effect.*

The aim of this work was to study the phase relations in the granite system Si-Al-Na-K-Li-F-O-H and the distribution of the main rock-forming and rare-earth elements between aluminosilicate (L) and aluminofluoride salt (LF) melts and water fluid (Fl) at a temperature of 800 to 600 °C, a pressure of 1 to 2 kbar and a water content of 2.5 to 48.96 wt. % H_2O. The compositions of the solid charge material for the experiments was set based on the composition of the aluminosilicate melt with defined ratios of Si, Al, Na+K+Li and the fluoride salt phase (cryolite) in an amount sufficient to saturate it the aluminosilicate melt. The initial composition of the silicate melt corresponded to granite eutectic system Qtz-Ab-Ort at 690 °C, 1 kbar H_2O, 1 wt. % F (Manning, 1981) and contained 1,5 wt. % Li.

The following reagents were used to prepare the initial compositions: LiF, K_2SiF_6, NaF, AlF_3, Al_2SiO_5, Al_2O_3, SiO_2 and distilled water. Rare earth elements (REE) La, Ce, Pr, Nd, Sm, Eu, Gd, Tb, Dy, Ho, Er, Tm, Yb and Lu, as well as yttrium (Y) and scandium (Sc) were introduced as oxides of 0,5 wt. % element's. The ratios of the reagents were chosen in such a way that the expected aluminosilicate melt in the products of the experiments was close to the compositions of highly evolved Li-F and cryolite-containing granites.

The experiments were carried out at the installation of high gas pressure ("gas bomb") at the Institute of experimental Mineralogy of the RAS in Chernogolovka (IEM RAS) in platinum ampoules. The size of the ampoules in length was up to 25 mm, outer diameter - 3 mm, wall thickness – 0.2 mm. Accuracy of temperature control and adjustment was ±5 °C; pressure ±50 bar. For each ampoule mass control was carried out before and after the experiment. The experiment was considered successful if the mass difference was no more than 0.001 g. The experimental products were investigated by scanning electron microscope Jeol JSM-6480LV (Japan) with energy dispersion INCA Energy-350 and crystal diffraction INCA Wave-500 (Oxford Instrument Ltd., Great Britain) spectrometer in the laboratory of local methods of substance research of the Department of Petrology of Moscow state University. The accelerating voltage was 20 keV at a current of 0.7 nA. Concentrations of rare earth elements and lithium were determined by inductively coupled plasma mass spectrometry on the ICP MS device in the laboratory of the MSU Department of Geochemistry.

As a result of the experiments, solid products of the experiments were obtained, represented by a tempered translucent glass (matrix) and hardened round globules of white color, consisting of small quenching crystals of alkali aluminofluorides and fluorides of REE, Y, Sc. Starting from ~ 10 wt. %, in the system there is a free aqueous fluid.

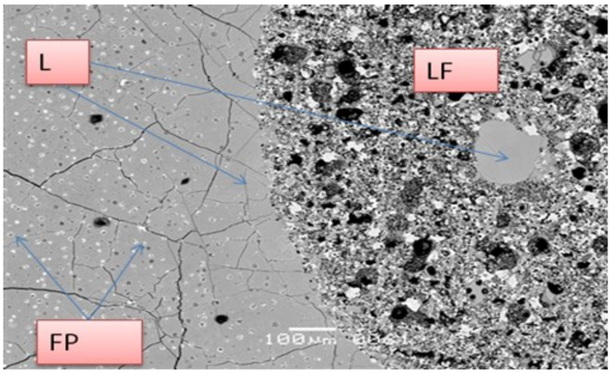

Fig.1. Hardening salt globul (LF) in the silicate matrix (L) with small hardening phases (FP) and the inclusion of silicate glass. Image in back-scattered electrons (in BSE).

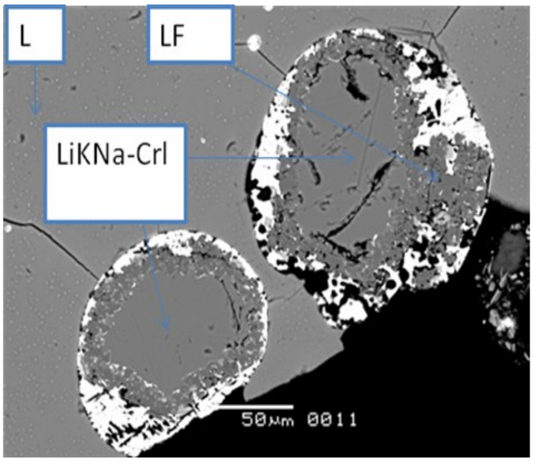

Fig. 2. Globules of salt melt, from which start to crystallize Li-K-Na crystals of cryolite (Lina-Crl), which is alyumoferritnoy residual melt (LF), concentrated fluorides of REE.

The obtained data on the phase relations in the system are shown in Fig. 1-3 as the temperature decreased from 800 to 600 °C. At a temperature of 800 °C and a pressure of 1 and 2 kbar, the system was in the liquidus region. Independently of the water content introduced into the system, the equilibrium phases were: aluminosilicate (L) and aluminofluoride salt (LF) melts and aqueous fluid (Fig.1). At 15 wt. % H_2O large pores in the molten salt reaching 20 µm and smaller pores in the silicate glass are visible. They indicate a high fluid content in both phases and, especially, in the salt. With a decrease in temperature to 700 °C, the phase relations changed, and the system moved to the subsolidus region. Alumosilicate and salt melts remained equilibrium, but Li-K-Na cryolite (Crl) began to crystallize from the aluminofluoride melt (Fig.2). At this temperature and pressure of 1 and 2 kbar, three types of globules were observed in the system. All fluorides in globules of the first type are distributed unevenly, representing areas, groups of small crystals, more enriched with either aluminum fluorides or fluorides of rare earths. The second type of globules is represented by smaller secretions of oval (length up to 180, width up to 80 µm) or round shape (50-100 µm in diameter) with more evenly distributed small quenching phases of fluorides. Their gross composition is close to the composition of the globules of the first type. In some samples globules of the third type are found (Fig.2), the main feature of which is the presence in their central part of the rounded crystals of K-Na aluminofluorides up to 100 µm, probably containing lithium, judging by the deficit of the amount of alkalis in the formula of this phase.

They are enclosed in the center of the salt globule and probably represent a single crystal, which during crystallization from the salt melt pushed it to the boundaries of the globules. The salt melt was enriched with the phases of rare earths. Increase water to 50 wt. % at T=700°C and P=2 kbar affected the shape of globules and the increase in pore size in both melts. Globules became oval, lenticular, crescent, etc. At the maximum water content in the system, the melt acquires "fluidity". The pores are often around the globules. Small elongated discharge of the salt phase "flow around" large globules.

When the temperature decreased by another 100 °C, the system remained in the subsolidus region, but the phase relations changed. The equilibrium phases at 600 °C and 1 kbar were aluminosilicate melt, quartz, aluminofluoride salt melt and Li-K-Na Crl (Fig.3). The last phase crystallized from the salt melt. The crystal size of the Crl was ~ 200 µm.

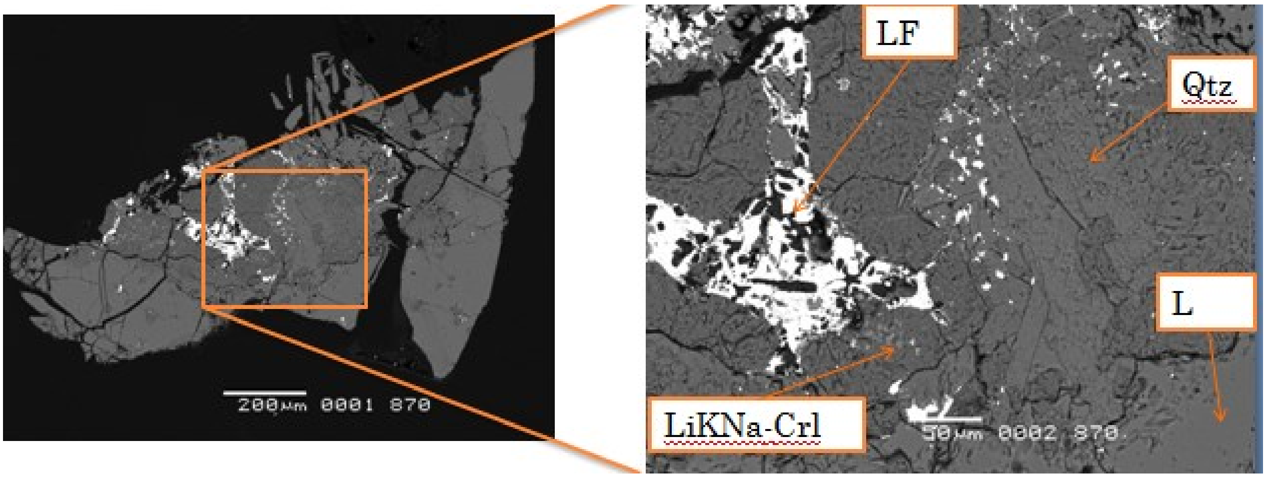

Fig. 3. The plot of the sample. Mineral equilibrium phases obtained at 600 °C and 1 kbar. Crystallization of Li-K-Na cryolite from salt melt (LF) and quartz (Qtz) from silicate melt (L) images in BSE.

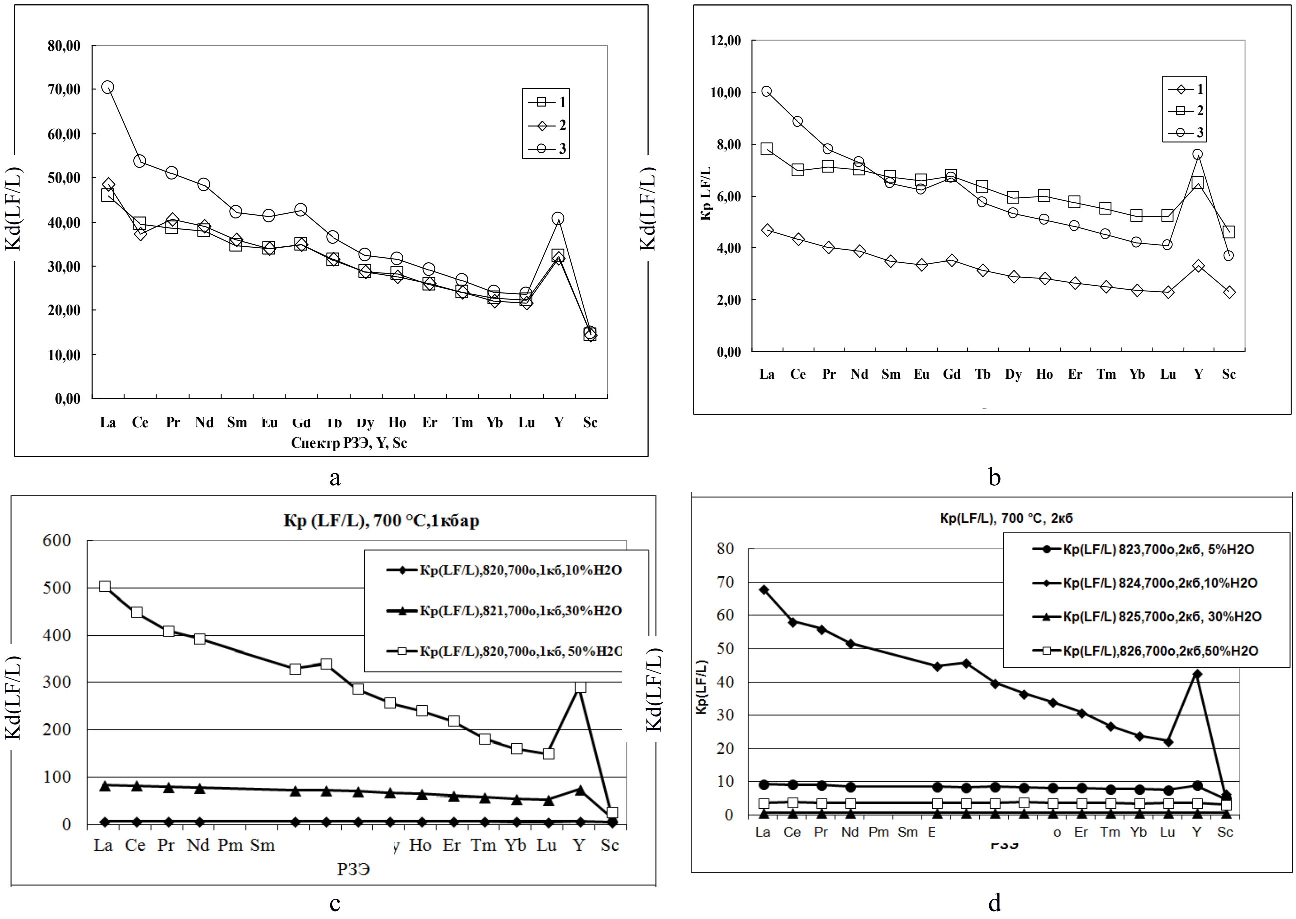

Fig. 4. The separation coefficients of REE, Y and Sc Kd(LF/L) between aluminofluoride and aluminosilicate melts: a - 800°C, 1 kbar, 1 - 2% H_2O, 2 – 5,4% H_2O, 3 – 10,3% H_2O; b - 800 °C, 2 kbar, 1 – 2,5% H_2O, 2 – 5,2% H_2O; 3 – 12,5% H_2O, b – 700 °C, 1 kbar, 1 – 10% H_2O, 2 – 30% H_2O, 3 – 50% H_2O; g – 700 °C, 2 kbar, 1 – 5% H_2O, 2 – 10% H_2O, 3 – 30% H_2O, 4 – 50% H_2O.

Another of the tasks of the work was to study the influence of temperature and pressure on the distribution of rare earth elements, scandium and yttrium, as well as on the main rock-forming elements. In work (Gramenitsky et al., 2005) it is shown that Si, Al, K and O are mainly distributed in aluminosilicate melt, and Al, Na, F – in aluminofluoride salt melt. In this work, the behaviour of the principal elements was studied at T=700 °C, P=1 and 2 kbar. To see a direct correlation between partition coefficients (Kd) between aluminofluoride and aluminosilicate melts (LF/L) content of water in the system: the KdK and KdSi at 1 kbar slightly increase, while KdAl reduced by 0.8. The KdNa and

KdF monotonically decreases. As the pressure increases to 2 kbar, the behavior of Na, Al and F changes. The partition coefficients of Na and F at concentrations of water up to 30 wt. % give the lowest values (5 and 6.8), and at 50 wt. % water – range of about 9. KdAl begins monotonically increase to a value of 1.6. KdK and KdSi decreased by 0.1. This is probably due to the beginning of crystallization of K-Na cryolite from aluminofluoride melt. And also, it is possible that with increasing pressure and water content, the structure of the silicate melt changes, contributing to the transition of the Al part from tetrahedral to octahedral coordination.

REE behavior depends on the temperature, pressure and water fluid content in the melt. According to the experiments carried out at 800 °C, there is a decrease in KdREE(LF/L) from light to heavy, both at 1 and at 2 kbar (Fig. 4a,b). Sc is always distributed in favor of an aluminosilicate melt, however, its low values of separation coefficients in comparison with rare earths indicate a relatively higher affinity of Sc to aluminosilicate melt, compared with most REE. And the separation coefficients of yttrium are greater than one, which indicates its greater affinity to the salt melt. Also, there is a tendency that as the water concentration in the system increases, the KdREE (LF/L) increases. When the temperature decreases to 700 °C, the separation coefficients increase (Fig.4b,d). There are differences in Kd depending on the water introduced into the system, but they are not natural. The tendency to decrease the coefficients of REE separation at 800 °C with an increase in pressure from 1 to 2 kbar is maintained. It is experimentally obtained that all rare earth elements, yttrium, scandium and lithium are distributed in favor of the salt aluminofluoride melt, regardless of the specified experimental conditions. The separation coefficients between salt and aluminosilicate melts at 2 kbar are significantly reduced compared to those for 1 kbar. According to ICP MS, the aqueous fluid is the most depleted phase in Li, REE, Sc and Y.

As a result of the new data obtained at lower temperatures, it is shown that the salt phase enriched with rare earth elements remains in equilibrium with the silicate melt and fluid up to a temperature of 600 °C at a pressure of 1 kbar. Quartz begins to crystallize from the silicate melt, and from the salt – phase of LiNaK - cryolite. Rare earth elements form fluorides of LnF3 composition or complex fluorides with alkaline elements during salt melt quenching.

As a result of the data obtained, the following conclusions were made:

1) It’s shown that when the temperature decreases from 800 to 600 °C, the phase composition of the system changes: at 700 °C, P = 1 and 2 kbar, a partial crystallization of the salt melt occurs with the formation of large crystals of aluminofluorides that practically do not contain rare earths. The residual salt melt, even more enriched with rare earth elements and casting, is stored in the system up to 600 °C. With a water content of more than 10 wt. % there was a free water fluid in the system.

2) At T = 600 °C and P = 1 kbar, quartz crystallizes from the aluminosilicate melt (L) and the phase composition of the system becomes: L+LF+Crl+Qtz.

3) Regardless of the given experimental conditions, all rare earth elements and lithium with large separation coefficients (several times) are distributed in a salt aluminofluoride melt.

4) REE separation coefficients between salt and aluminosilicate melts depend on temperature, pressure and volatile (water) content in the system.

5) Experimental data confirm the assumptions (Gramenitsky et al., 2005, Alferieva et al., 2011, Shchekina et al., 2013) about the formation of cryolite-containing granites at late stages of formation of large granite massifs as a result of separation from magma of salt alkaline fluoride melts rich in rare elements and capable of crystallizing much later than aluminosilicate melt at lower temperatures.

The work was supported by the Russian Foundation for Basic Research, grant No. 16-05-00859.

References:

Alferyeva Ya.O., Gramenitsky E.N., Shchekina T.I. Experimental study of phase relations in the lithium bearing fluorine-rich gaplogranite and nepheline-syenite systems. Geochemistry (7). 2011. P. 713-728 (in Russian).

Gramenitsky E.N., Shchekina T.I., Devyatova V.N. Phase relations in fluorine-containing granite and nepheline-syenite systems and distribution of elements between phases. Moscow: GEOS. 2005. P. 186 (in Russian).

Shchekina T.I., Gramenitsky E.N., Alferyeva Ya.O. Leucocratic magmatic melts with fluorine limit concentrations of fluorine: experiment and natural relations. Petrology 21 (5). 2013. P. 499 – 516 (in Russian).

Manning D. The effect of Fluorine on liquidus phase bonds in the system Qz-Ab-Or with excess water at 1 kb // Contrib. Mineral. Petr. V. 76. 1981. pp. 206-215.

Shchekina T.I.[1], Rusak A.A.[1], Alfereva Ya.O.[1], Gramenitsky Ye.N. [1], Kotelnikov A.R.[2], Zinovieva N.G.[1], Bychkov A.Yu.[1], Akhmedzhanova G.M.[2] The role of lithium in the differentiation of granite melts with extreme concentrations of fluoride and distribution of rare earth elements at a

pressure of from 1 to 5 kbar UDC 552.11, 550.42.

[1]Lomonosov Moscow State University, Department of Geology, Russia, Moscow, [2] Institute of Experimental Mineralogy RAS, Russia, Chernogolovka (t-shchekina@mail.ru, aleks7975@yandex.ru; *yanaalf@yandex.ru*, engramen@geol.msu.ru, kotelnik@iem.ac.ru, nzinov@mail.ru, andrewbychkov@rambler.ru, akhm@iem.ac.ru). 119991, Russia, Moscow, Lenin Hills, 1, aud. 607. +7 (495) 939-20-40.

Introduction to the model granite system Si-Al-Na-K-F-O-H lithium in an amount of about 2 at.% at 800 ºC and 1 kbar leads to the appearance of a wide area of incompressibility between aluminosilicate and LiKNa-aluminofluoride (salt) melts in the system (Gramenitsky et al., 2005; Alferyeva et al., 2011). It is shown that the salt melt enriched with lithium in comparison with silicate is stable at 800 °C in the pressure range from 1 to 5 kbar and up to 600 ºC at 1 kbar. Rare earth elements, yttrium and scandium, along with lithium, accumulate with high separation coefficients >>1 in the salt melt in the range of 800 – 600 ºC at 1 kbar. They remain in it until its complete crystallization in the form of complex compounds of REE, Y and Sc, forming fluorides and LiKNa-fluorides during quenching. It was found that the pressure increase from 1 to 5 kbar leads to the convergence of the concentrations of Li, REE, Y and Sc in silicate and salt melts and a significant decrease in their separation coefficients.

***Keywords**: lithium; granite system; rare earths; separation factor; aluminosilicate; aluminofluoride; salt melts; water content; influence of pressure.*

The main mechanism of differentiation in the magmatic process considered in Petrology and Geochemistry of elements is the mechanism of crystallization differentiation with fractionation of crystalline phases. This mechanism does not explain a number of processes occurring in granite melts at the latest stages of their differentiation. This refers to the melts from which ongonites, elvans, Li-F and cryolite-containing granites and their pegmatites are formed. They are enriched with fluorine and often lithium – incompatible elements that undoubtedly affect the formation of these rocks. Our experiments are aimed at explaining the Genesis of such rocks and the associated ore concentrations of rare elements. At the first stage of experimental work in the model granite system, Si-Al-Na-K-Li-F-O-H (Gramenitsky et al., 2005), we set ourselves the task of obtaining a silicate melt saturated with water and fluorine as an analogue of pegmatite magma in the assumption that it will be separated from granite magma by the mechanism of liquid incompressibility. We have not obtained such a silicate melt. With an increase in the fluorine content of more than 3 wt. % we consistently obtained alkaline-aluminium-fluoride phases corresponding to the composition of K-Na cryolite (Crl or Cry) on the liquidus of the system. Only in a narrow high-alumina region of the compositions of the system was found a salt fluoride melt, equilibrium with silicate, close in composition to the chiolite. Introduction to the Li system (in an amount of more than 1 wt. %) led to a significant expansion of the field of the salt melt in the system by reducing the field of cryolite (Alfereva et al., 2011). Aluminum fluoride melt, has a variable composition depending on the part of the system. The ratio of Al/Na in it ranges from 20/80 to 40/60. We had been delineated by an extensive region of immiscibility in the system Si-Al-Na-Li-F-O-H. An experimental study of the system showed that for the explanation of the origin of pegmatites and leucocratic, rich in fluorine and lithium species, inevitably the involvement of physico-chemical systems involving not only fluid (volatile), and salt components. The mechanism of liquid incompressibility in natural systems can play a significant role in the differentiation of granite melts. In the 2000s, there was an increased interest in experimental work in this area due to the detection of salt melts in melt inclusions in granitoid minerals (Badanina et al., 2006; Andreeva et al., 2007; Solovova et al., 2010). In this paper (Peretyazhko et al., 2010) melt of cryolite and fluorite composition is described in inclusions. Inclusions of silicate-salt melts were also obtained in artificial inclusions in minerals (Kotelnikova, Kotelnikov, 2008). Largely due to the study of melt inclusions, magmatic deposits now include large rare-metal deposits of Zashikhin and Katuginskoye, which are confined to cryolite-containing granites. Previously, they were fully or partially ranked as metamorphogenic-metasomatic. We believe that all manifestations of cryolite-containing granites, including the exclusive Ivigtut Deposit and smaller formations, should be attributed to magmatic ones with the participation of fluoride melts during their differentiation (Shchekina T. et al, 2013). Salt and, in particular, high-fluoride aqueous fluids and fluoride melts are of particular importance in explaining the nature of the distribution of rare earth elements in the differentiation of granite magmas and subsequent metasomatosis and ore formation in granites (Irber, 1999, Gusev A.I., Gusev A.A., 2011).

In this paper, special attention is paid to the behavior of lithium in the silicate-salt high-fluoride system Si-Al-Na-K-Li-F-O-H. Along with fluorine, lithium manifests itself as an important element that affects the phase relations in the system and provides a manifestation of the liquation separation of the salt melt from the aluminosilicate. Its influence on the distribution of rare-earth elements between melts is known (Gramenitsky, Shchekina, 2005; Veksler, 2005). Before this work the task was to investigate the influence of pressure on the nature of the distribution of Li between the silicate and salt phase and the distribution of rare earth elements between them.

Conditions and methods of experiments. The initial materials for the experiments were a fluoride-silicate mixture consisting of chemical reagents SiO_2, NaF, LiF, AlF_3, Al_2O_3, K_2SiF_6, and distilled water. Rare earth elements La, Ce, Pr, Nd, Sm, Eu, Gd, Tb, Dy, Ho, Er, Tm, Yb, Lu, as well as Y and Sc were introduced into the system in the form of oxides of 0.5 wt.% element's. The experiments were carried out on the installation of high gas pressure with internal heating. The duration of the experiments was 5-7 days. Platinum ampoules with a diameter of 3 mm were used as containers for the substance of the experiments. Experimental conditions: temperature 800 ° C and pressure 1, 2, 3 and 5 kbar. The experiments were carried out with a certain reference composition of the model granite, similar in composition to granite eutectic at 1 kbar and 4 mass. % F (Manning D., 1981), under H2O saturation conditions. The experiments also differed in the content of injected water from 2 to 50 %. The study of phase relations and chemical composition of solid products of the experiments was carried out in the Laboratory of local methods of substance research of the Department of Petrology of the geological faculty of Moscow state University. Electronic images are obtained in the mode of reflected electrons (BSE). Analysis of the main elements and fluorine in phases was performed using a scanning electron microscope Jeol JSM-6480LV (Japan) with energy dispersion Oxford X-MaxN and crystal diffraction INCA Wave-500 (Oxford Instrument Ltd., UK) spectrometers. Shooting conditions: voltage 20 kV, current 0.7 nA. The accuracy of the estimation of the main elements in the synthesized phases was 2 – 5 comparative %. Instrument error in the measurement of fluorine was ±1 % of the element concentration. In a number of samples the main and rare-earth elements in silicate glasses were studied using the electron probe microanalyzer Superprobe JXA-8230 (Japan). Analysis of rare earth elements, Y, Sc and Li was performed by inductively coupled plasma mass spectrometry in the laboratory of experimental Geochemistry of the Department of Geochemistry of the geological faculty of Moscow state University. Measurements were carried out on a mass spectrometer with ionization in inductively coupled plasma with double focusing Element-2. The measurement error was 1-3 comparative %.

Conclusion. The study of phase relations showed that at a temperature of 800 °C, a pressure of 1-5 kbar and a different water content from 2 to 50 wt. % is the balance of two melts aluminosilicate (L) and aluminofluoride (salt LF). With a water content of more than 10 mass.% the fluid phase is in equilibrium with two melts, that is the system passes to the 3-phase equilibrium. It is macroscopically seen that the increase in water content contributes to a significant increase in porosity and increase in the size of the pores themselves, especially in silicate melts. Increasing the pressure to 5 kbar leads to a more uniform distribution of quenching REE fluorides in the globules of the salt phase. The content of Li in the silicate phase ranged from ~ 1 to 1.5 wt. %, and salt - from 1 to 11 wt. %. The separation coefficients in all experiments exceed 1, i.e. Li is always distributed mainly in the salt phase (Fig.1a).

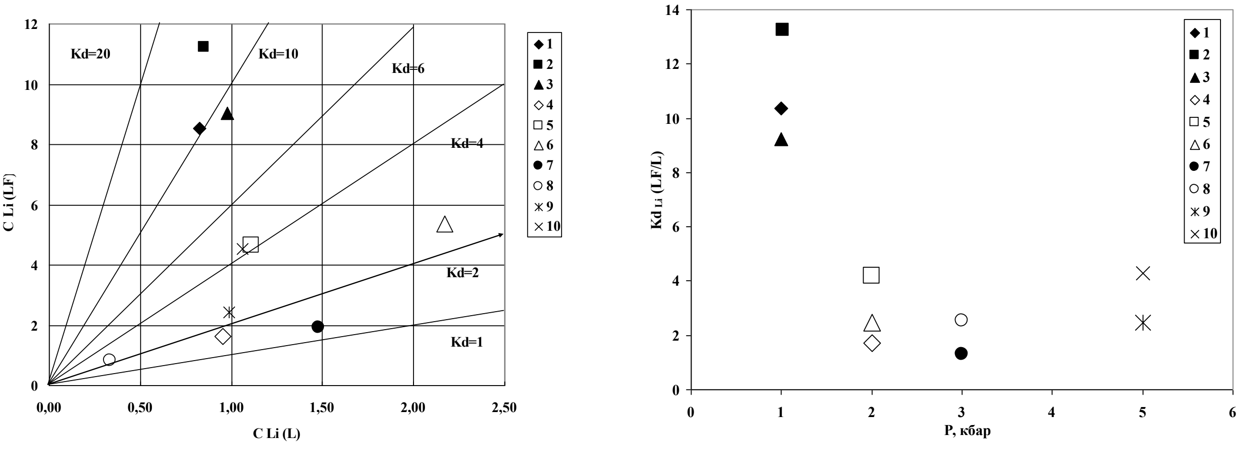

a *b*

Fig. 1. a. The distribution of Li (wt. %) between aluminosilicate (L) and salt (LF) melts at 800 °C, 1 - 5 kbar. Symbols: experiment numbers at 1 kbar pressure– 1 - 776, 2 – 778, 3 – 777 with 2,06, 5,12 and 9,3 wt. % H_2O, respectively; at a pressure of 2 kbar– 4 – 785, 5 – 786, 6 – 787 with 2,4, 4,9, 11,1 wt. % H_2O, respectively; at a pressure of 3 kbar – 7 - 817, 8 – 718 with 30 and 50 wt. % H_2O, respectively; at a pressure of 5 kbar – 9 - 811, 10 - 812 with 5 and 10 wt. % H_2O, respectively. Lines correspond to the partition coefficients (LF/L) is equal to from 1 to 16. b. The dependence of the lithium separation coefficients KdLi(LF/L) between the salt and silicate melts on the pressure from 1 to 5 kbar at T=800 °C. The designations are the same as in Fig. 1a.

In the experiments carried out with 1кбар, observed the most high (8,5-11,2 wt. %) Li concentrations in the salt phase compared with experiments at higher pressures at water content in the system from 2.06 to 9, 34 wt. %. Li concentrations in aluminosilicate glass in experiments at 1 kbar not higher than 1 wt. %, while in samples obtained at higher pressures, it reaches 1.5-2 wt.%. Accordingly, the lithium separation coefficients $Kd_{Li}^{(LF/L)} = C_{Li}^{LF}/C_{Li}^{L}$, where the C_{Li}^{LF} - concentration of Li in the salt melt and the C_{Li}^{L} - concentration of Li in the silicate melt are significantly higher for samples obtained at a pressure of 1 kbar (from 9.23 to 13.24) than at higher pressures. Points corresponding to pressures 2, 3 and 5 kbar (Fig. 1a) overlap and occupy the field in the interval between Kd=1 to Kd=4. Thus, it was found that the separation coefficients of Li decrease with increasing pressure (Fig.1b).

The study of the distribution coefficients of rare earth elements, yttrium and scandium between salt and silicate melts showed that they have a direct relationship with the nature of lithium distribution. For fig.2 it can be seen that the higher $Kd_{Li}^{(LF/L)}$, the higher $Kd_{REE, Y, Sc}^{(LF/L)}$.

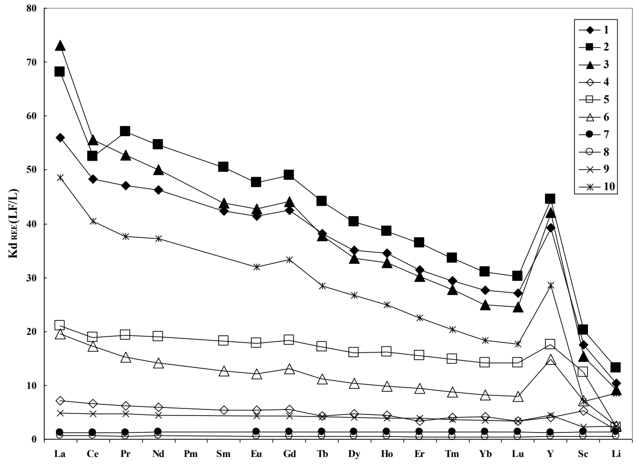

Fig. 2. Dependence of separation coefficients $Kd_{REE, Y, Sc}^{(LF/L)}$ and $Kd_{Li}^{(LF/L)}$ between salt and silicate melts on pressure at 800 °C. Designations as in Fig. 1 a,b.

The highest coefficients of separation of REE, Y and Sc are typical for experiments at 1 kbar. Their spectra are located at the top of the graph (Fig.1b). Below are the spectra for the experiment at 5 kbar and 10 % H_2O, then the spectra of samples obtained at 2 kbar with different water contents and the spectrum at 5 kbar and 5 % H_2O and below all – spectra at 3 kbar. More research is needed to explain these data. However, the trends in the distribution of elements in all experiments are similar. The shape of REE, Y and Sc spectra has a great similarity. The separation factors decrease relatively smoothly from light to heavy REE, forming a small maximum in the Gd region. Yttrium manifests itself as a light REE, and Sc – like heavy. There is a dependence on the water content in the system, but it is not natural. It should be noted that against the background of weak changes in the composition of silicate and salt melts, depending on the pressure, rare earth elements and lithium react to changes in pressure and water content. Our data confirm that the entry of Li into the granite system acts in the same direction as fluorine and water, providing, apparently, a decrease in the viscosity of the melt and a decrease in the temperature of its crystallization. New results are obtained indicating a decrease in the coefficients of separation of REE, Y, Sc and Li between the salt and silicate melts with increasing pressure in the system. It is assumed that the presence of three components in the system – H_2O, F and Li causes a change in the structure of the silicate melt, contributing to the transition of part Al from tetrahedral to octahedral coordination, and this, apparently, affects the distribution of rare elements. Trivalent rare-earth elements, Y and Sc are readily included in the salt aluminum fluoride melt, forming complex compounds with F and probably c Li. The undoubted fact of Li influence on the phase relations, namely, the appearance of a wide area of incompressibility between silicate and salt melts in the granite system, determines its great influence on the behavior of rare elements.

Summary.

1. It is shown that the equilibrium of aluminosilicate and aluminofluoride (salt) melts in the model granite system was found at a temperature of 800 °C and 1 kbar, 4-10 mass.% H_2O, stored up to a pressure of 5 kbar at a water content of 2 to 50 wt. %.
2. The separation coefficients of rare earth elements, yttrium and scandium between salt and silicate melts increase with increasing lithium separation coefficients.
3. Increasing the system pressure from 1 to 5 kbar reduces the separation coefficients of REE, Y, Sc and Li between the salt and silicate melts.

The work was supported by the Russian Foundation for Basic Research, grant No. 16-05-00859.

References:

Alferyeva Ya.O., Gramenitsky E.N., Shchekina T.I. Experimental study of phase relations in the lithium bearing fluorine-rich gaplogranite and nepheline-syenite systems. Geochemistry (7). 2011. P. 713-728 (in Russian).

Andreeva I.A., Kovalenko V.I., Yarmolyuk V.V., Listratova E.N., Kononkova N.N. Incidence of silicate and salt (Li, Na, F) melts in the comendits of the occurrence of the Dzarta-Huduk (central Mongolia): data of the study of melt inclusions.

Doklady Earth Science. 414 (4). 2007. P. 528-534 (in Russian).

Gramenitsky E.N., Shchekina T.I., Devyatova V.N. Phase relations in fluorine-containing granite and nepheline-syenite systems and distribution of elements between phases. Moscow: GEOS. 2005. P. 186 (in Russian).

Kotelnikova Z.A., Kotelnikov A.R. NaF-bearing fluids: experimental study at T = 500-800 °C and P = 2000 bar by the synthetic fluid inclusion method in quartz. Geochemistry (1). 2008. P. 54-68 (in Russian).

Peretyazhko I.S., Savina E.A. Tetrade-effects in the spectra of distributions of rare earth elements of granitoid as the indicator of the fluoride-silicate liquid incidence in the magmatic systems. Petrology 18 (5). P. 536-566 (in Russian).

Solovova I.P., Girnis F.A., Kovalenko V.I. Liquid incidence in the system pantellerite liquid-F-Cl. Doklady Earth Science 433 (3). 2010. P. 390-393 (in Russian).

Shchekina T.I., Gramenitsky E.N., Alferyeva Ya.O. Leucocratic magmatic melts with fluorine limit concentrations of fluorine: experiment and natural relations. Petrology 21 (5). 2013. P. 499 – 516 (in Russian).

Badanina E. V., Trumbull R. B., Dulski P., Wiedenbeck M., Veksler I. V., Syritso L. F. The behavior of rare earth and lithopile trace elements in rare-metal granites: a sudy of fluorite, melt in clutions and host rocks from the Khangilay complex, Transbaikalia, Russia. Can. Mineral. 44. 2006. P. 667-692.

Irber W. The lanthanide tetrad effect and its correlation with K/Rb, Eu/Eu*, Sr/Eu, Y/Ho, and Zr/Hf of evolving peraluminous granite suites. Geochim. Cosmochim. Acta63 (3/4). 1999. P. 489-508.

Manning D. The effect of Fluorine on liquidus phase relationships in the system Qz-Ab-Or with excess water at 1 kb // Contrib. Mineral. Petr. V. 76., 1981. P. 206-215.

Veksler I. V., Dorfman a.m., Kamenetcky M., Dulskii P., Dingwell D. B. Partitioning of lanthanides and Y between immiscible silicate and fluoride melts, fluorite and cryolite and the origin of the lanthanide tetrad effect in igneous rocks. Geochim. Cosmochim.Acta 69 (11). 2005. P.2847-2860.

Suk N.I. Interphase distribution of elements in silicate-phosphate systems UDC 550.89:553.062

Institute of Experimental Mineralogy RAS (IEM RAS), (sukni@iem.ac.ru)

Abstract. The results of an experimental study of liquid immiscibility occurring in alkaline silicate-phosphate systems at T = 1250°C and P=2 kbar under water pressure are presented. The experiments were carried out in high gas pressure vessel. The distribution of petrogenic and ore elements between silicate and phosphate melts was studied. It is shown that the phosphate melt concentrates Ca, Mg and Na, the nature of the separation of Al and K between silicate and phosphate melts depends on the initial composition of the system, decreasing with increasing ratios (Ca+Mg)/(Na+K) and (Ca+Mg)/(Si+Al) of silicate melt. High efficiency of phosphate extraction was revealed in relation to REE, Ti, Nb, Ta, W, Sn. The partition coefficients of zirconium vary from 2.15 to 0.76, decreasing with an increase in the ratio Ca/(Na+K) and Ca/(Si+Al) and an increase in agpaiticity ((Na+K)/Al) of silicate melt.

Keywords: *liquid immiscibility, silicate melt, phosphate* ***melt****, experiment, elements distribution*

The liquid immiscibility that occurs in alkaline silicate-phosphate systems and the distribution of petrogenic and ore elements between silicate and phosphate melts has been experimentally investigated.

The experiments were carried out on a high gas pressure vessel at T = 1250 ° C and P = 2 kbar under dry conditions and in the presence of water (12% **by** weight of the sample). The compositions of model systems were specified by mixtures of natural minerals (nepheline, albite, diopside, potassium feldspar, apatite) and $NaPO_3$. Ore components were added in the form of oxides of rare-earth elements, Ti, Zr, Nb, Ta, as well as Na_2SnO_4 and Na_2WO_4. The obtained samples were analyzed on a Camebax X-ray microanalyzer (Cameca, France) with a Link AN-10000 energy dispersive spectrometer (Oxford Instruments, England).

In the systems studied, wide field of splitting into two immiscible liquid phases – silicate and alkali-phosphate melts, which form either droplets of one melt in another, or stand out in the form of a layer with a clear phase boundary between melts, were established (Fig. 1). Experiments conducted in dry and water-containing systems demonstrate an inversion of densities: dissolving a fluid in a phosphate melt leads to a decrease in its specific gravity compared to a silicate melt, as a result of which the salt melt floats up, which in this case is located in the upper part of the sample (Fig. 1).

The compositions of coexisting liquids are well illustrated by the diagram in coordinates (Na_2O + Al_2O_3) – P_2O_5 – SiO_2. Fig.2 shows the liquid immiscibility areas of melts for the various systems studied (Suk, 1993). These data reflect a narrowing of the liquid separation zone when CaO and MgO are added to the alkaline melt in diopside composition, which indicates an increase in the mutual solubility of phosphate and aluminosilicate melts (Fig. 2a, c) and is consistent with the data (Delitsyna et al., 1989). The same trend is observed when adding the first percent of TiO_2 to the system (Fig. 2b). A regular change in the compositions of coexisting melts is observed: the more the salt component is contained in the system, the more acidic the immiscible silicate phase has.

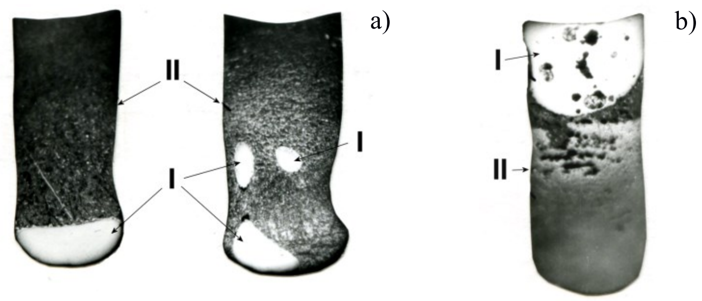

Fig. 1. Liquid immiscibility in silicate-phosphate system (T=1250°C, P=2 kbar) with the formation of layers: a - under water pressure; b - in the dry system. I - silicate melt; II - phosphate melt. Sample thickness is 2.8 mm.

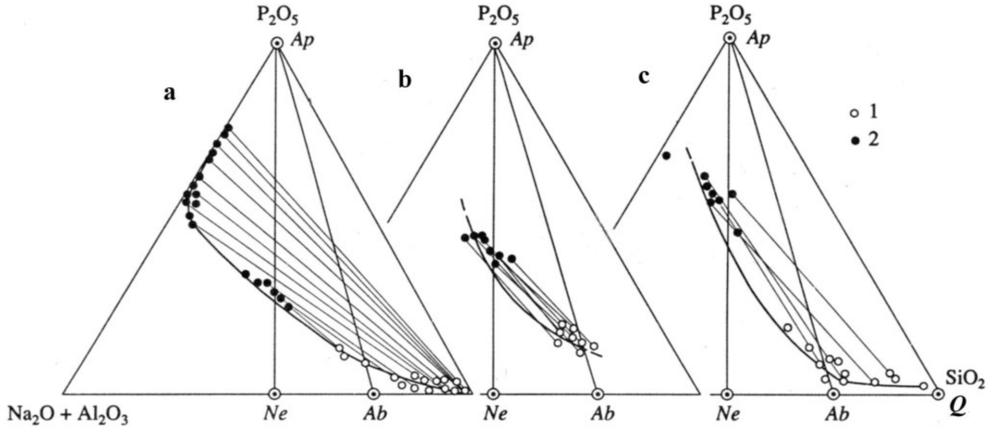

Fig. 2. Liquid immiscibility region in the systems: (a) – albite – apatite – $NaPO_3$ – H_2O; (b) – albite – apatite – TiO_2 – $NaPO_3$ – H_2O; (c) – albite – diopside – $NaPO_3$ – H_2O according to experimental data at T=1250°C, P=2 kbar (wt.%). 1, 2 – compositions of coexisting melts.

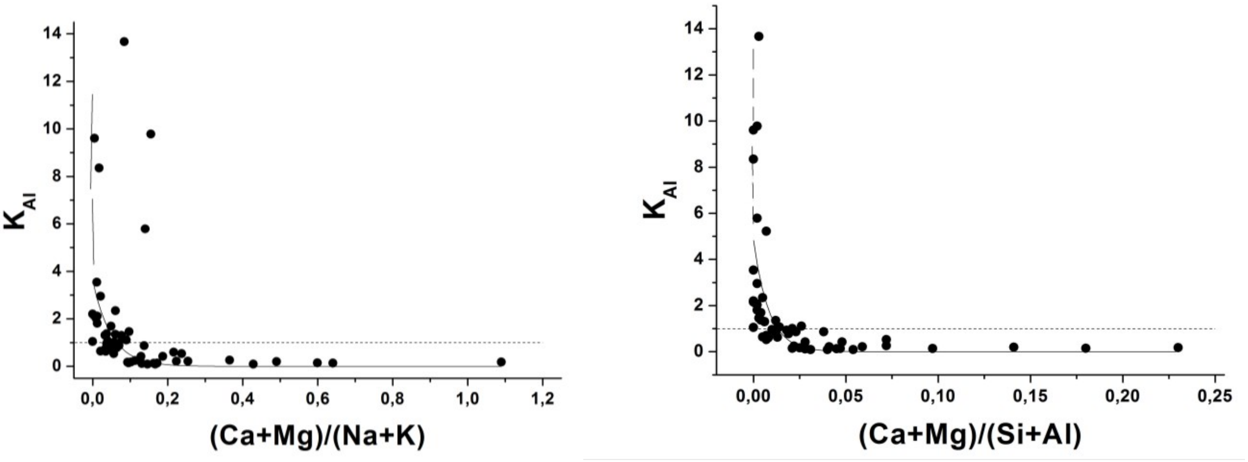

a

b

Fig. 3. The dependence of the partition coefficient of aluminum (KAl) on (Ca+Mg)/(Na+K) (a) and (Ca+Mg)/(Si+Al) (b) of silicate melt.

As a result, there is a separation of elements between the phases, while Ca, Mg, Na are concentrated in the phosphate melt.

In the systems SiO_2 – Al_2O_3 – Na_2O – K_2O – P_2O_5, the phosphate melt is enriched in alumina (Suk, 1991). The partition coefficient ($K = C_{Al2O3}^{ph} / C_{Al2O3}^{sil} > 1$), depending on the composition of the system varies from 1.1 to 13.6.

The addition of Ca, Mg, and Ti to the system promotes the redistribution of Al into a silicate liquid ($K = C_{Al2O3}^{ph} / C_{Al2O3}^{sil} < 1$). The partition coefficient depending on the composition of the system varies from 0.98 to 0.1. Thus, the dependence of the Al_2O_3 partition coefficient between silicate and phosphate melts on the initial composition of the system, which correlates with the compositions of the resulting immiscible phases, is revealed. The partition coefficients decrease with increasing ratios of (Ca + Mg) / (Na + K) and (Ca + Mg) / (Si + Al) in silicate melt (Fig. 3), as well as with increasing agpaiticity. These dependencies can be described by the following equations:

$K_{Al}=\exp(1.28687(\pm0.044) - 20.01268(\pm1.578)*X)$, where X=(Ca+Mg)/(Na+K), the error in estimating K_{Al} by this equation is $E_x=0.053$;

$K_{Al}=\exp(1.57304(\pm0.041) - 119.42(\pm11.374)*X)$, where X=(Ca+Mg)/(Si+Al), $E_x=0.078$.

These equations work well with significant contents of CaO and MgO, up to $K_{Al}\approx5$.

The concentration of Al_2O_3 in silicate liquid is accompanied by an increase in the relative content of Na_2O in it and a slight decrease in the SiO_2 amount. This character of separation seems to be related to the structural position of Al in coexisting melts: in silicate melt Al, replacing Si in a silicon-oxygen tetrahedron, is in quadruple coordination, and in phosphate melt it is also present in the sixth coordination (Delitsyna, Delitsyn, 1991).

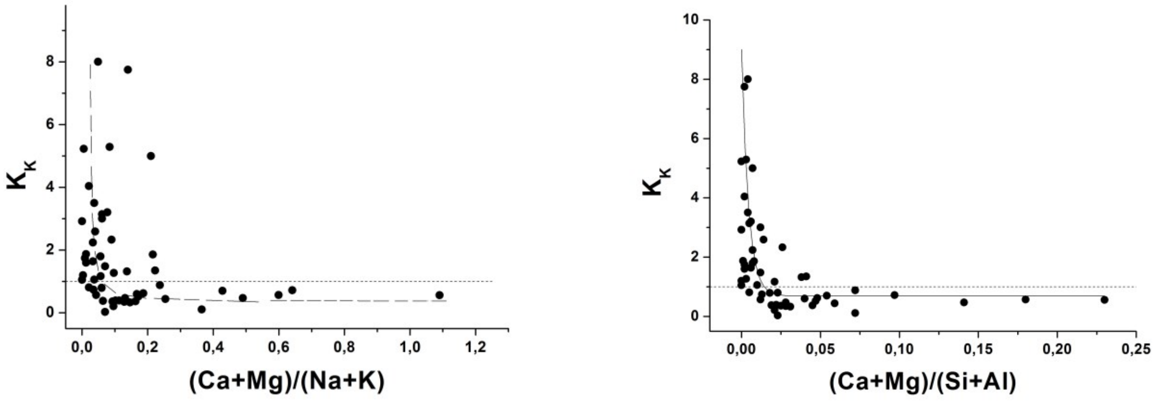

a

b

Fig. 4. The dependence of the partition coefficient of potassium (KK) on (Ca+Mg)/(Na+K) (a) and (Ca+Mg)/(Si+Al) (b) of silicate melt.

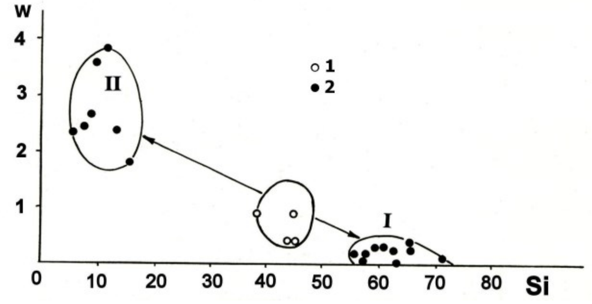

Fig. 5. The distribution of tungsten and silicon between the layered phases in silicate-phosphate systems (at.%). 1 – initial compositions of samples, 2 – compositions of layered phases.

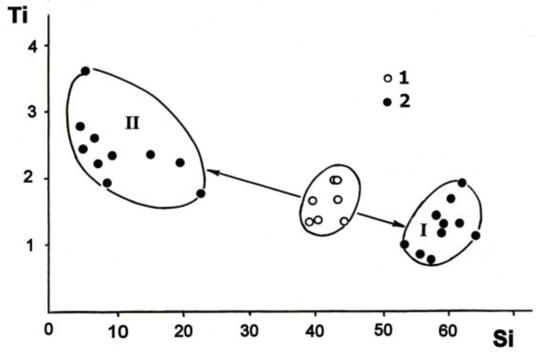

Fig. 6. The distribution of titanium and silicon between the layered phases in silicate-phosphate systems (at.%). 1 – initial compositions of samples, 2 – compositions of layered phases.

In potassium-containing systems, a regular separation of K and Na is observed between the coexisting layering phases (Suk, 1991). When the initial melt is splitted into silicate and phosphate phases (in the systems $SiO_2 – Al_2O_3 – Na_2O – K_2O – P_2O_5$, when $K=C_{Al2O3}^{ph}/C_{Al2O3}^{sil}>1$), a concentration of K and Na occurs in the phosphate melt ($K=C_{Na2O}^{ph}/C_{Na2O}^{sil}$ and $K = C_{K2O}^{ph}/C_{K2O}^{sil}>1$). In systems containing Ca, Mg and Ti, where $K=C_{Al2O3}^{ph}/C_{Al2O3}^{sil}<1$, potassium mainly passes into aluminosilicate liquid (with partition coefficient $K=C_{K2O}^{ph}/C_{K2O}^{sil} <1$), and Na – into phosphate, where $K=C_{Na2O}^{ph}/C_{Na2O}^{sil}>1$. Thus, sodium in all cases predominantly concentrates in the phosphate melt, and the nature of potassium separation depends on the initial composition of the system, which correlates with the compositions of the resulting immiscible phases. Partition coefficients decrease with increasing ratios of (Ca+Mg) / (Na+K) and (Ca+Mg)/(Si+Al) of silicate melt (Fig. 4), as well as with increasing agpaiticity. These dependencies can be described by the following equations:

$K_K=35.75413(\pm5.047)*$
$*\exp[X/(-0.01296)(\pm0.001)]+0.4748(\pm0.170)$, where $X=(Ca+Mg)/(Na+K)$, $E_x=0.411$;
$K_K=8.31295(\pm0.561)*$
$*\exp[X/(-0.0043)(\pm0.0007)]+0.68958(\pm0.248)$, where $X=(Ca+Mg)/(Si+Al)$, $E_x=0.176$.

These equations are applicable with significant contents of CaO and MgO, up to $K_K \approx 5$.

The distribution of tungsten and tin between the layered phases was studied at T = 1100 and 1250 ° C and P = 2 kbar in the presence of water (12 wt.% by weight). The results show that phosphate melt has a higher content of W (Fig. 5) than silicate melt (Suk, 1997). The partition coefficient of W depending on the initial composition of the system varies from 7.7 to 28.8.

In the distribution of Sn between the phases, the observed contrast is not as sharp as in the case of W:

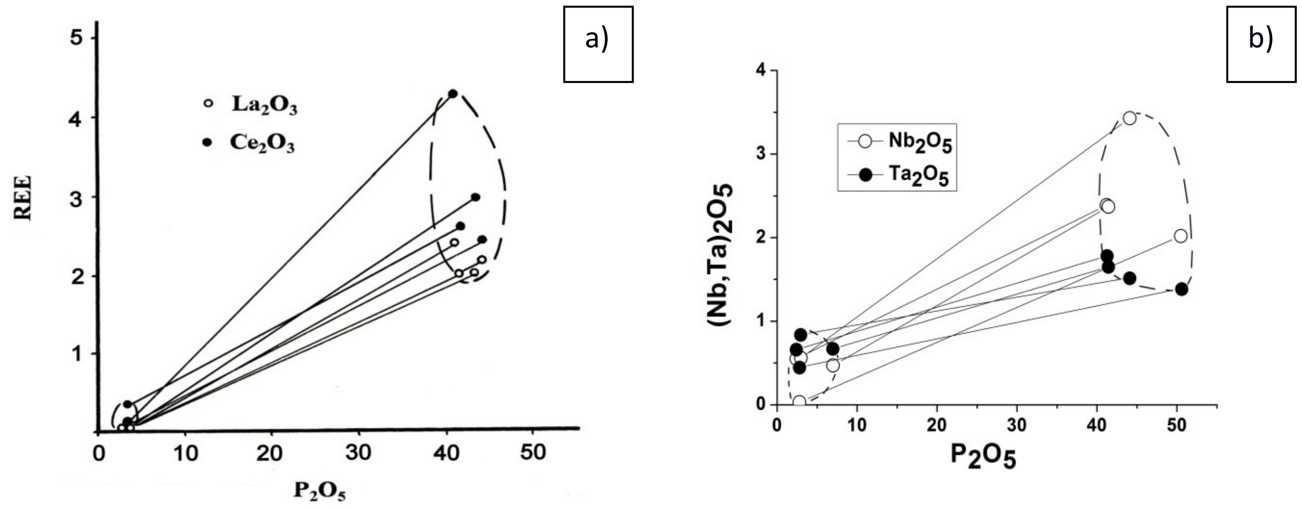

Fig. 7. The distribution of rare-earth elements and phosphorus (a) and niobium, tantalum and phosphorus (b) between the layered phases in silicate-phosphate systems (wt%).

the partition coefficient $K = C_{SnO2}^{ph}/ C_{SnO2}^{sil}$ is 1.36-4.63.

The study of the behavior of titanium in layering silicate-phosphate systems at T=1250°C, P=2 kbar in the "dry" and water-containing systems shows the preferential extraction of titanium into the phosphate melt (Fig. 6). According to experimental data, $K = C_{TiO2}^{ph}/C_{TiO2}^{sil}$ is 2-3.4, which confirms the close paragenetic bond of phosphorus with titanium.

The data on the distribution of rare-earth elements between the immiscible silicate and phosphate phases at T=1250°C and P=2 kbar show that rare earths (La, Ce) are concentrated in the phosphate melt (Fig. 7a) (Suk, 1997). At the same time, their partition coefficients ($K=C_{REE}^{ph}/C_{REE}^{sil}$) are much more than one.

The distribution of niobium and tantalum was studied in the “dry” system Ab – Di – $NaPO_3$ – Nb_2O_5 – Ta_2O_5 at T=1250°C, P=2 kbar. Experimental results show that niobium and tantalum are predominantly concentrated in the phosphate phase (Fig. 7b), their partition coefficients ($K=C^{ph}/C^{sil}$) are always greater than one (Suk, 1998a): for Nb - from 4 and higher, for Ta – 1.8-3.1.

The distribution of zirconium was studied in the “dry” system Ab – Di – $NaPO_3$ – ZrO_2 at T=1250°C, P=2 kbar at various ratios of minerals in the initial mixture. The dependence of the partition coefficients of Zr between silicate and phosphate melts on the initial composition of the system, which correlates with the compositions of the resulting immiscible phases, is revealed. The partition coefficients ($K_{Zr} = C_{Zr}^{ph}/C_{Zr}^{Sil}$) vary from 2.15 to 0.76, decreasing with increasing Ca/(Na+K) and Ca/(Si+Al) ratios and increasing agpaiticity ((Na+K)/Al) of silicate melt. These dependencies can be described by the following equations (Suk, 2017):

K_{Zr}= 2.84376(±0.236) – 37.06152(±6.618)*X, where X = Ca/(Na+K), the error in estimating K_{Zr} by this equation is E_x=0.154;

K_{Zr}= 2.7646(±0.136) – 138.78862(±15.063)*X, where = Ca/(Si+Al), E_x=0.094.

Conclusions

1. It was shown that phosphate melt concentrates Ca, Mg and Na, the nature of the separation of Al and K between silicate and phosphate melts depends on the initial composition of the system, decreasing with increasing ratios of (Ca+Mg)/(Na+K) and (Ca+Mg)/(Si+Al) of silicate melt.

2. High efficiency of phosphate extraction was revealed in relation to REE, Ti, Nb, Ta, W, Sn. The partition coefficients of zirconium vary from 2.15 to 0.76, decreasing with an increase in the ratio Ca (Na+K) and Ca/(Si+Al) and an increase in agpaiticity ((Na+K)/Al) of silicate melt.

References:

Delitsyna L.V., Delitsyn L.M., Pavlov E.G. et al. The immiscibility of the liquid phases in the system $Ca_5(PO_4)_3F$ – SiO_2 – NaF – CaO – MgO and its significance in the genesis of apatite ores // Dokl. Earth Sci.of the USSR. 1989. T. 305. No. 1. P. 162-166.

Delitsyna L.V., Delitsyn L.M. The immiscibility of the liquid phases in the $Ca_5(PO_4)_3F$ – SiO_2 – NaF – Al_2O_3 system and its significance in the genesis of apatite deposits // Dokl. Earth Sci.of the USSR. 1991. T. 317. No. 4. P. 963-967.

Suk N.I. Experimental studies of liquid immiscibility of phosphorus-containing feldspathoid melts // Dokl. Earth Sci.of the USSR. 1991. T. 316. N 6. P. 1461-1464.

Suk N.I. Liquid immiscibility in phosphorus-containing melts in connection with the genesis of apatite deposits (experimental studies). // Petrology. 1993. T. 1. N 3. P. 282-291.

Suk N.I. Behavior of ore elements (W, Sn, Ti and Zr) in layering silicate-salt systems // Petrology. 1997. V. 5. N 1. P. 23-31.

Suk N.I. Liquid immiscibility in alkaline magmatic systems. 2017. M.: “KDU”, “University Book”. 238 p.

Zharkova E.V., Lukanin O.A., Tsekhonya T.I. Redox conditions of formation of olivines and basalts from various geodynamic zones based on electrochemical measurements of the intrinsic oxygen fugacity UDC 550.843 (543.559)

V.I. Vernadsky Institute of Geochemistry and Analytical Chemistry RAS, Moscow (zharkova@geokhi.ru, lukanin@geokhi.ru, tsekhonya@geokhi.ru)

Abstract. We used an electrochemical method based on two solid electrolyte cells to measure the intrinsic oxygen fugacity (fO_2) of olivines and island-arc basalts from Kamchatka, as well as MORB basalts from the Atlantic Ocean and the Red Sea. The measurements were carried out at 1 atm in the temperature range of 800°C to 1150°C. The temperature dependence of fO_2 obeys the Nernst law and can be described by a linear equation as the following form: $\log fO_2 = A - B/T$°K. The fO_2 values of basalts are between the wustite-magnetite (WM) and quartz-fayalite-magnetite (QFM) buffers, increasing with increasing temperature. The fO_2 of basalts becomes ≥ fO_2 (QFM) at extrapolation to the subliquidus temperature range at the beginning of their crystallization (1150-1250°C). The highest $\log fO_2$ (≈ QFM+1) are characteristic of the high-magnesium basalts of the Tolbachik volcanic zone of Kamchatka. In general, our results are in good agreement with available estimates obtained using various mineral oxybarometers. Measured fO_2 for olivines from allivalite deep inclusions in Kamchatka basalts compared to basalts have lower values that are close to or practically coincide with fO_2 (WM) over the entire temperature range. Variations of basalts and olivines fO_2 reflect changes in the redox regime during the evolution of primary magmas during their crystallization in magmatic chambers at different depths.

Keywords: *the intrinsic oxygen fugacity, basalts, olivine, electrochemical method, solid cell.*

Introduction. Oxygen fugacity (fO_2) as well as temperature and pressure are an important factor determining the processes of evolution of mantle magmas during their ascent to the surface, crystallization and degassing. Estimates of fO_2 values in magmatic systems can be obtained by calculation methods using various mineral oxybarometers or experimentally by electrochemical determination of the intrinsic oxygen fugacity of minerals and mineral associations of igneous rocks.

This report presents the results of the electrochemical determination of the intrinsic oxygen fugacity for olivines and basalts of active volcanoes of Kamchatka and MORB type basalts from the Atlantic Ocean and Red Sea. The obtained data are compared with the available estimates of the fO_2 formation of basalt magmas of Kamchatka and oceanic rifts performed by other methods.

Table 1. Chemical composition of basalts

Oxides (wt.%)	L–21	TL-10-08-76	T–6	P-57	DIX-QT
SiO_2	52.05	51.20	51.2	50.1	49.51
TiO_2	0.82	1.71	1.40	0.84	1.66
Al_2O_3	15.16	17.60	16.30	16.2	14.68
Fe_2O_3	4.48	2.58	3.59	1.93	1.78
FeO	5.16	8.21	6.53	7	8.66
MnO	0.10	0.16	0.17	0.16	0.19
CaO	9.29	7.94	6.78	13.4	8.33
MgO	9.48	4.50	9.26	7.9	10.88
Na_2O	2.46	3.26	2.00	1.71	3.11
K_2O	0.89	2.00	1.56	0.08	0.17
P_2O_5	0.13	0.63	0.40	0.04	-
H_2O^-	0.03	0.07	-	0.25	0.38
H_2O^+	0.06	0.13	0.13	-	-
Total	100.12	99.99	99.32	99.65	99.35

Methods and samples. The fO_2 measurements were carried out on a high-temperature installation using two electrolytic cells at 1 atm in the temperature range from 800°C to 1150°C. The use of two cells allows determining $fO2$ for minerals and mineral associations with low oxygen buffer capacity. The studied samples (fragments of rocks and monomineral fractions of olivines) were carefully selected under a microscope so that they did not have any signs of a secondary change. A more detailed procedure for sample preparation and measurement of $fO2$ is given in (Kadik, Zharkova et al., 1989).

Two samples of basalt of the Great fissure Tolbachik eruption of 1975-1976 (Kamchatka) (high-Mg (T-6) and high-Al (TL-10-08-76) compositions) and one sample of high-Mg basalt from Kluchevskoi volcano, Kamchatka (L-21), as well as tholeitic basalts of the MORB type from the Atlantic Ocean (DIX-QT) and the rift zone of the Red Sea (P-57) were studied. The chemical compositions of basalts are presented in table 1. In addition, measurements of fO_2 were carried out for three samples of olivines from deep allivalite inclusions in low-calcium-alkaline basalts of Kamchatka: Ilyinsky (Cu-41), Mutnovsky (B-621a), and Ksudach volcanoes (Ka-77/7). Allivalite, coarse-grained olivine-anortite rocks, are supposed to be genetically related to host basalt and are products of early crystallization of basalt magmas in volcanic chambers at different depths (Burikova, Parfenova, 2013). All allivalite inclusions from which olivines were taken were covered with basalt film. Microprobe analyses of olivines are presented in table 2.

Table 2. Microprobe analyses of olivines from allivalite inclusions in basalts of Kamchatka and from mantle xenoliths in alkaline basalts of Mongolia (ShTs Z-1), Baikal rift zone (P 664 A) and Tian-Shan (Kch-9)

Oxides (wt.%	Cu – 41	B - 621 a	Ka – 77/7	ShTs Z-1	P 664 A	Kch-9
SiO_2	40.09	39.15	39.33	41.01	40.94	41.62
MgO	43.80	41.74	41.44	48.15	48.07	50.92
Al_2O_3	0.07	0.00	0.00	-	-	0.01
CaO	0.17	0.21	0.22	0.04	-	0.01
TiO_2	0.02	0.03	0,02	0.00	-	0.02
$FeO+Fe_2O_3$	15.63	19.64	19.60	10.74	9.98	6.82
MnO	0.27	0.31	0.27	0.11	0.15	0.12
Cr_2O_3	0.02	0.00	0.01	0.00	0.00	0.06
V_2O_3	0.00	0.00	0.03	0.02	0.00	0.00
NiO	0.09	0.01	0.08	0.37	0.37	0.48
CoO	0.03	0.01	0.09	-	-	0.04
Total	100.19	101.10	101.09	100.44	99.51	100.1
Fo	83.00	78.84	78.74	88.44	89.09	92.46
Fa	17.00	21.16	21.26	11.56	10.91	7.54

Results and discussion. The results of determination the intrinsic oxygen fugacity of basalts at different temperatures are presented in Fig. 1 and 2. The temperature dependence of fO_2 for all basalts obeys the Nernst law and can be described by a linear equation of the form: $\log fO_2 = A - B/T(K)$, where A and B are constants (Table 3).The $\log fO_2$ values of the basalt samples studied in the range of 800-1150°C are located in the region between the wustite-magnetite (WM) and quartz-fayalite-magnetite (QFM) buffer equilibria, approaching to the QFM buffer line with increasing temperature. The extrapolation of the temperature dependence to the crystallization temperatures of the liquidus mineral phases (1150-1250°C) shows that fO_2 for basalts L-21 and TL-10-08-76 becomes equal to or exceeds fO_2 (QFM), and for basalt T-6 it can reach Ni-NiO buffer values (Fig. 1, Table 3). The difference of fO_2 between basalts at these temperatures is about 0.9-0.7 log units.

The obtained values of fO_2 can characterize the redox state of basalt melts at temperatures near the liquidus, if the crystallization of basalts and their complete solidification occurred in conditions that are closed to oxygen. The relatively high fO_2 for high-Mg basalt T-6 of the Tolbachik eruption 1975 at subliquidus temperatures (~ QFM + 1) generally agrees well with the available fO_2 estimates for these basalts, based on the composition of olivine phenocrysts and the ratio FeO/MgO in the melt (Lukanin et al., 1980), and also using a Cr-spinel-olivine oxybarometer (Mironov, Portnyagin, 2018).

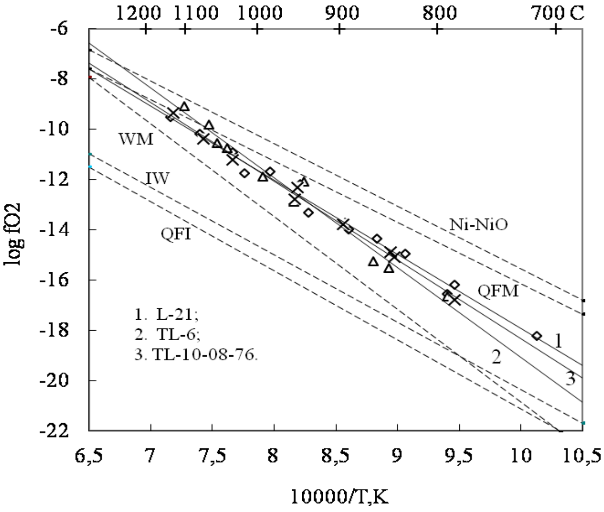

Fig 1. The dependence of $\log fO_2$ against $10^4/T°K$ for the basalts from Kamchatka region.

It should be noted that for high-Al basalts of the Tolbachik eruption, which are genetically associated with high-Mg basalts, the fO_2 values in the subliquidus temperature range are noticeably lower (~ QFM ± 0.2), which also agrees with the previously made fO_2 estimates for these basalts (Lukanin et al., 1980). A decrease in fO_2 probably reflects a change in the redox regime during the differentiation of primary high-Mg basaltic magmas during their crystallization and mixing of magma derivatives in the open magmatic system (Lukanin et al., 1991, Portnyagin et al., 2015).

The fO_2 values for MORB basalts DIX-QT and P-57 are almost identical over the entire studied temperature range (Fig.2). They correspond to fO_2 (QFM) at near-liquidus temperatures. This is consisted (within the accuracy of the approaches used) with the available estimates of fO_2 for basalts of this type in terms of the ratio Fe^{2+}/Fe^{3+} in basalt glasses, as well as in the Cr-spinel-olivine oxybarometer (Mironov, Portnyagin, 2018).

Measurements of the intrinsic oxygen fugacity of olivine of allivalite inclusions in Kamchatka basalts also demonstrate a clear linear relationship $\log fO_2 = A - B/T^oK$ (Fig. 3, Table 4). Compared to basalts, the studied olivine samples have lower fO_2 values, which are close (Ka–77/7) or practically coincide (Cu-41, B-621) with WM buffer over the entire temperature range. At sub-liquidus temperatures (1150-1250°C) the difference in fO_2 olivine and basalt is about 1-2 log units. This seems to reflect more reducing conditions during the crystallization of allivalites in deep-seated magmatic chambers.

Table 3. The values of the coefficients "A" and "B" in the empirical equation $\log fO_2 = A – B/T°K$ for the basalts of the Kamchatka, Atlantic Ocean and Red Sea

Sample	A	B	r	n	$\log fO_2$ at 1250°C	$\Delta QFM = \log fO_2(samp.) - \log fO_2(QFM)$
L-21 Kluchevskoi volcano	11.553	29484	0.988	11	-7.81	-0.05
TL-10-08-76 Tolbachik eraption	13.02	31358	0.994	9	-7.57	0.19
T–6, basalt, Tolbachik eraption	16.663	35762	0.979	11	-6.82	0.94
DIX-QT Atlantic ocean	14.097	32925	0.993	11	-7.52	0.24
P-57 Red Sea	13.08	31705	0.988	12	-7.73	0.03

r –coefficient of correlation; n – number of experimental points

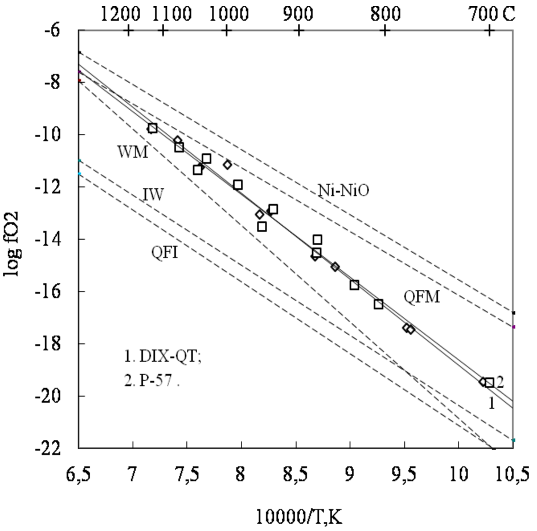

Fig. 2. The dependence of $\log fO_2$ against $10^4/T^oK$ for the MORB basalts from Atlantic Ocean and Red Sea.

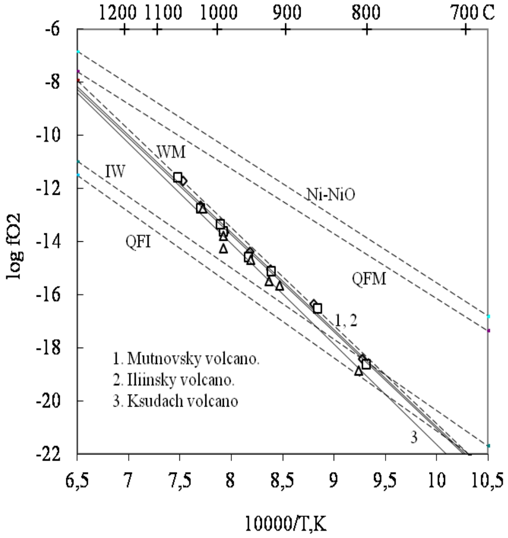

Fig. 3. The dependence of $\log fO_2$ against $10^4/T^oK$ for olivines from the Kamchatka region

Table 4. The values of the coefficients "A" and "B" in the empirical equation $\log fO_2 = A - B/T°K$ for the olivines olivines from allivalites and mantle xenoliths

Sample	A	B	r	n	$\log fO_2$ at 1250°C	$\Delta QFM = \log fO_2(sam) - \log fO_2(QFM)$
Cu-41 Iliinsky volcano	15.488	36540	0.993	8	-8.50	-0.74
B-621a Mutnovsky volcano	15.603	36591	0.995	8	-8.42	-0.66
Ka-77/7 Ksudach volcano	16.184	37832	0.983	7	-8.66	-0.9
ShTs Z-1 (Kadik, Zharkova et al., 1989)	10.804	30887	0.996	10	-9.45	-1.69
P-664A (Kadik, Zharkova et al., 1994)	12.507	33126	0.986	8	-9.24	-1.48

Sample	A	B	r	n	log fO_2 at 1250°C	ΔQFM = logfO_2(sam)-logfO_2(QFM)
Kch-9 (Kadik, Zharkova et al., 1995)	15.260	37832	0.994	7	-9.58	-1.82

r - coefficient of correlation; n - number of experimental points

Additionally, in Table 4, the results of measurements of the intrinsic oxygen fugacity of olivine from mantle xenoliths in alkaline basalts of continental rifts (Mongolia, Baikal Rift Zone, Tien Shan) are shown in the form of analytical dependence of logfO_2 vs 1/T (Kadik et al., 1989, 1994, 1995). Microprobe analyses of olivines are given in table. 3. At high temperatures (1250°C), the fO_2 values for these olivines are approximately on 1 log unit is lower compared to fO_2 olivines from allivalites. These data may reflect the redox regime in even deeper areas of primary alkaline basaltic magmas formation.

Conclusion

1. The fO_2 values of Kamchatka island-arc basalts and MORB type basalts. measured by the electrochemical method in the range of 800-1150 ° C. are located between the WM and QFM buffers and are described by the linear dependence in the form: log fO_2 = A - B/T°K. At temperatures close to the liquidus (1150-1250 ° C) fO_2 basalts become ≥ fO_2 (QFM). The highest fO_2 at these temperatures are characteristic of the high-Mg basalts of the Tolbachik eruption Kamchatka (~ QFM + 1).

2. Estimates of the redox state of the studied basalts at near-liquidus temperatures, based on measurements of the intrinsic oxygen fugacity, generally agree well with the available calculated fO_2 for these basalts obtained by various methods including Cr-spinel-olivine oxybarometers.

3. Olivines from allivalite inclusions in basalts of Kamchatka volcanoes have at subliquidus temperatures the fO_2 values on 1-2 orders of magnitude lower as compared to basalts. This is a reflection of more reducing conditions during crystallization of basaltic melts in deep-seated volcanic chambers.

The investigation was carried out under partly support of RFFI No17-05-00713 and Program No 17.

References:

Burikova I. A. and Parfenova O. V. 2013. Allivalites as Indicators of Fractional Crystallization of the Island-Arc Calc-Alkaline Low-K Series. *Geochemistry International.* V. 51. No. 1. P. 33-43.

Kadik A.A., Zharkova Ye.V., Kovalenko V.I., Ionov D.A. 1989. Upper Mantle Redox Conditions: Oxygen Fugacity Measurement on Peridotite Xenoliths from the Shavaryn Tsaram Volcano. Mongolia. *Geochemistry International.* V. 26. No 1. P. 12-19.

Kadik A.A., Zharkova He.V., Kiselev A.I. 1994. Baikal Rift Zone Spinel and Garnet Lerzholite Redox State. *Doklady of Russian Academy of Science.* V. 337. P. 100-103.

Kadik A.A., Zharkova E.V., Lutkov V.S., Tadgibaev G.T. 1995. Redox Conditions of Mantle Xenoliths from South and Middle Tian-Shan. *Geochemistry International*. No 8. P. 1094-1099.

Lukanin O. A., Kadik A. A., Biggar G. M., Fedotov S. A. 1980. Physico-Chemical Conditions of Crystallization of Basalts of the Great Tolbachik Fissure Eruption 1975-1976. *Volcanology and Seismology.* No 3. P. 16-50 (in Russian).

Lukanin O. A., Kadik A. A., Borisov A.A. 1991. Petrogenesis of Basalts of the Tolbachik Eruption in 1975-76 on Kamchatka and Some Problems of High-Aluminum Basalt Magmas Formation in Regions of Island arc. *Geochem. International.* V. 28. No 8. P. 90-112.

Mironov N. L., Portnyagin M. V. 2018. Coupling of Redox Conditions of Mantle Melting and Copper and Sulfur Contents in Primary Magmas of the Tolbachinsky Dol (Kamchatka) and Juan de Fuca Ridge (Pacific Ocean) *Petrology.* Vol. 26. No. 2. P. 145–166.

Portnyagin M., Duggen S., Hauff F., Mironov N., Bindeman I., Thirlwall M., Hoernle K. 2015. Geochemistry of the Late Holocene Rocks from the Tolbachik Volcanic Field. Kamchatka: Quantitative Modelling of Subduction-Related Open Magmatic Systems. *Journal of Volcanology and Geothermal Research*. V. 307. P. 133–155.